Engineering of the Musculoskeletal System and Rehabilitation

3.2 Numerical methods

Shoulder

Shoulder biomechanics

- 4 bones: humerus, scapula, clavicle, thorax
- 4 joints (shoulder girdle)
- 20 muscles, divided in multiple sections
- 3x(3+3) degrees of freedom
- Constraints
- Soft tissues (ligaments)
- Proprioception mechanism
- Individual variability
- **Indeterminate system**

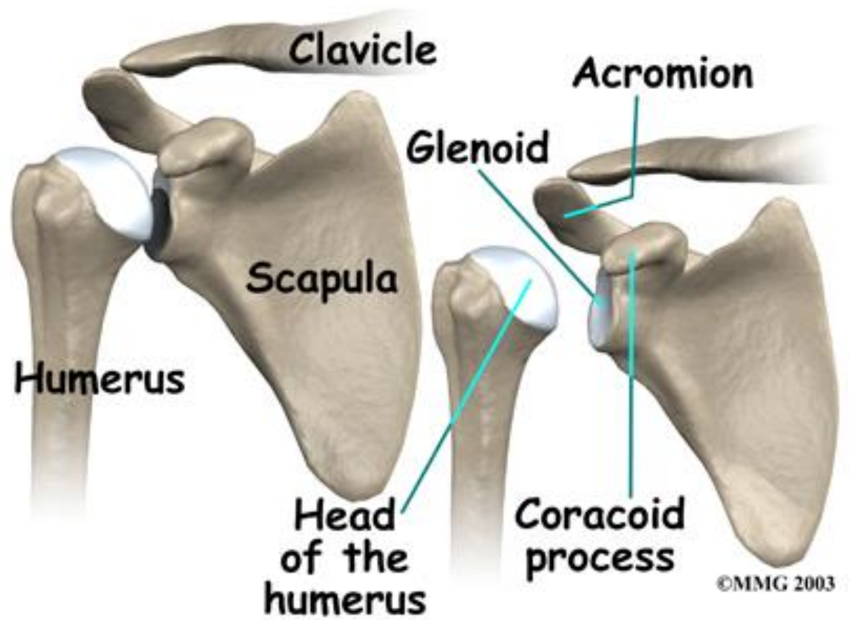

Rocking horse effect

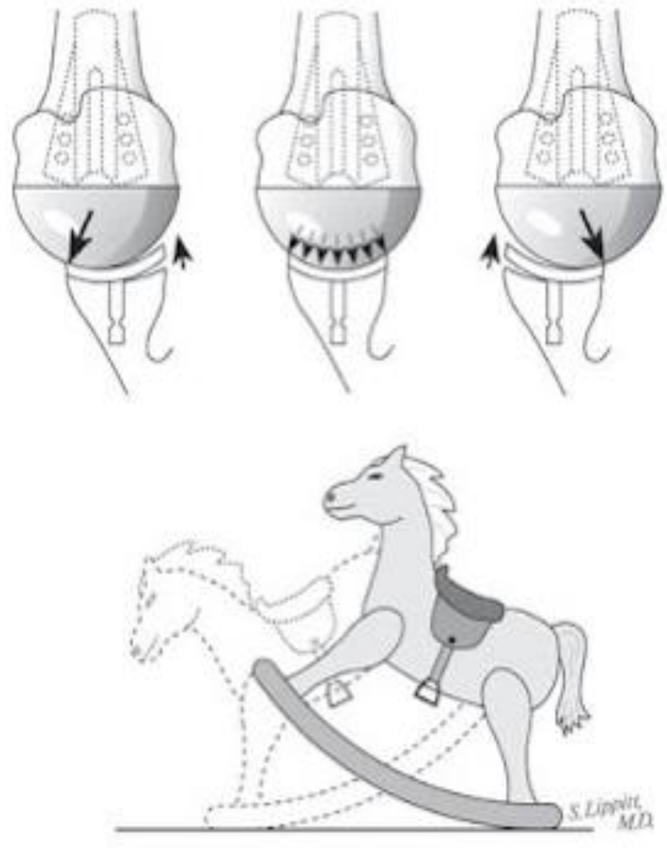

http://shoulderarthritis.blogspot.ch/2011/05/shoulder-joint-replacement-minimizing.html

Rocking horse effect

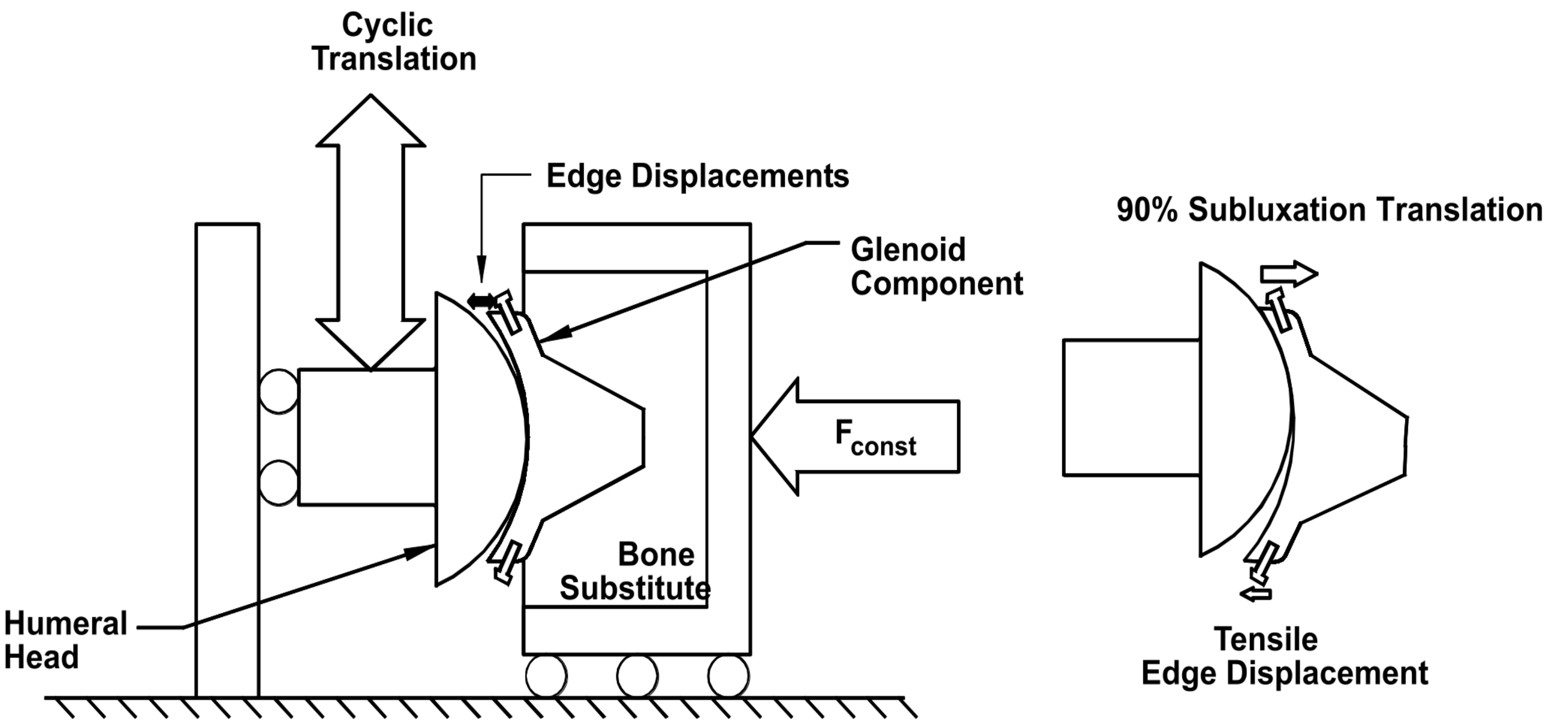

C. Anglin et al. / Clinical Biomechanics 16 (2001) 144-150

ASTM F2028-00 : Standard test method for the dynamic evaluation of glenoid loosening or disassociation

ASTM F1829 – 98: Standard Test Method for Static Evaluation of the Glenoid Locking Mechanism in Shear

2D model

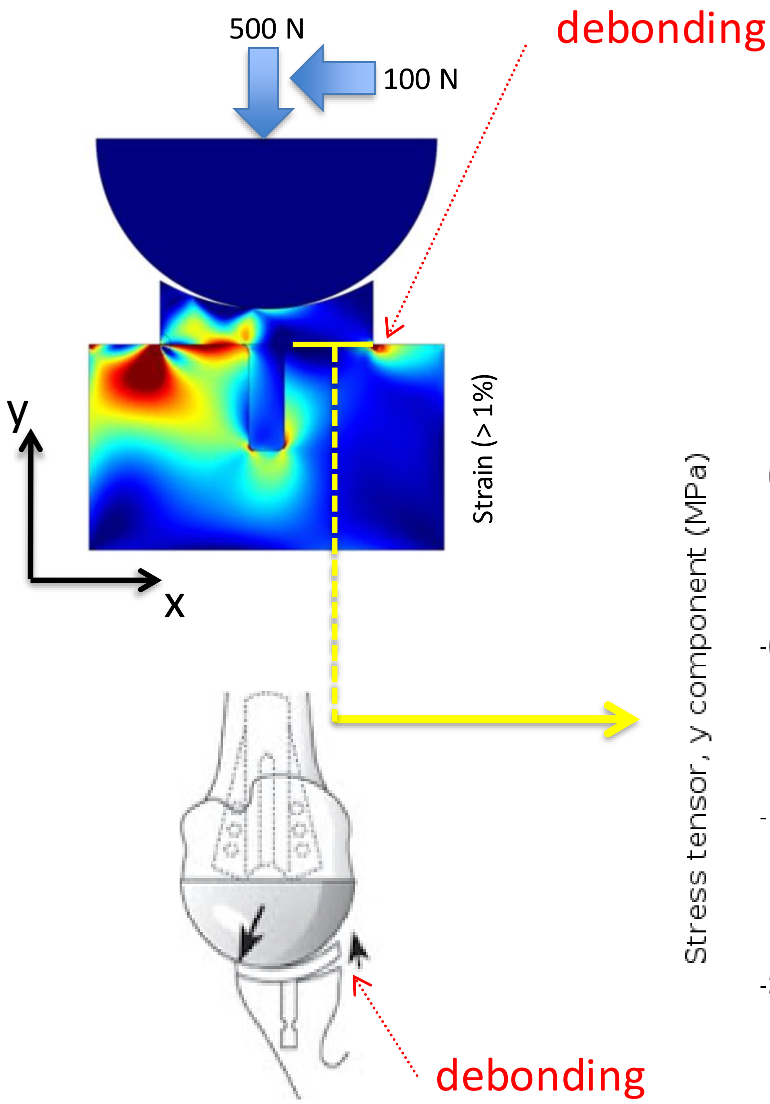
500 N
100 N
debonding
Strain (> 1%)
y
x
debonding

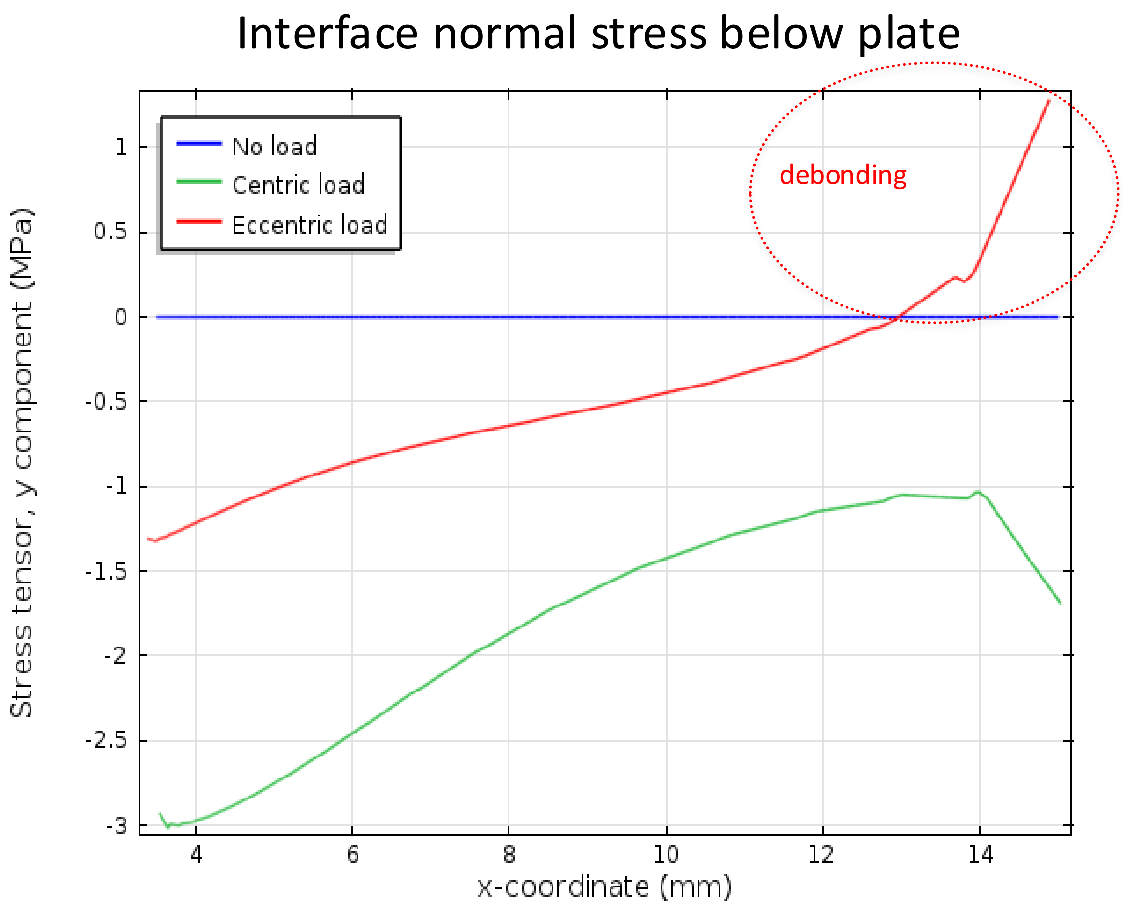
Interface normal stress below plate
No load
Centric load
Eccentric load
debonding
Stress tensor, y component (MPa)
x-coordinate (mm)
1
0.5
0
-0.5
-1
-1.5
-2
-2.5
-3
4
6
8
10
12
14

Model requirement

- Perform active and loaded movement
- Predict joint forces
- Predict pressure contact pattern with joint
- Predict stress within cartilage, bone, **prostheses**
- **Predict humeral head translation**
- Consistent with current knowledge (models, cadaveric, clinical)

→ **indirect validation**

Musculoskeletal model

- Focus on gleno-humeral joint
- Allow humerus translation
  - Avoid the ball-and-socket assumption
- Use EMG data as muscular ratios
  - Avoid unknown EMG-force relationship
  - Avoid co-contraction problem of optimization

2D algebraic model

- Ball-socket joint: only 1 degree of freedom
- Include scapulo-humeral rhythm
- Account for muscles-humerus contact
- Indeterminate: **fixed muscles forces ratio**
  - F2/F1=r1, F3/F1=r2, …
- Solve equilibrium equations
  - Muscles forces
  - Glenohumeral reaction force
    (orientation → contact location)

2D algebraic model

- F_1 : Deltoid medium (humerus contact)
- F_2 : Deltoid anterior, deltoid posterior
- F_3 : Supraspinatus (humerus contact)
- F_4 : Infraspinatus, subscapularis

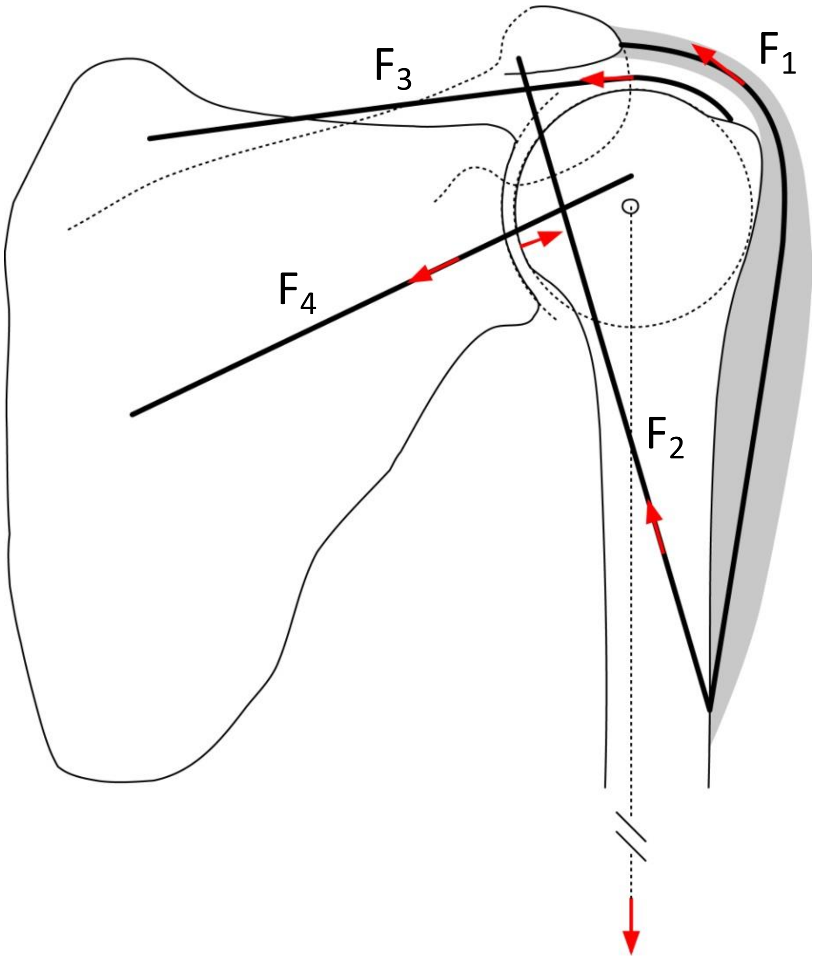

Constant muscular force ratio

Muscle forces introduced as relative to MD

- Ratios estimated from literature
- Averaged for the entire movement

$$F_m = F_{MD} \cdot R_m$$

$$R_m = PCSA_m \cdot EMG_m$$

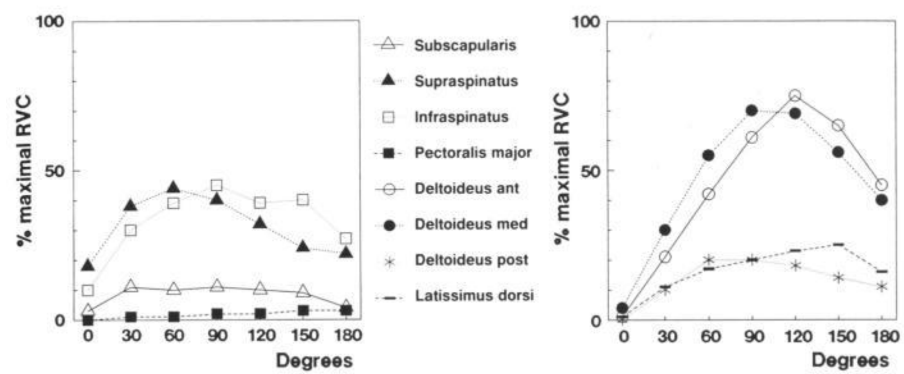

	MD	AD	PD	SS	SC	IS
PCSA	1.0	1.0	1.0	0.5	1.5	1.5
EMG	1.0	0.8	0.2	1.0	0.3	0.3
Ratios	1.0	0.8	0.2	0.5	0.5	0.5

2D algebraic model

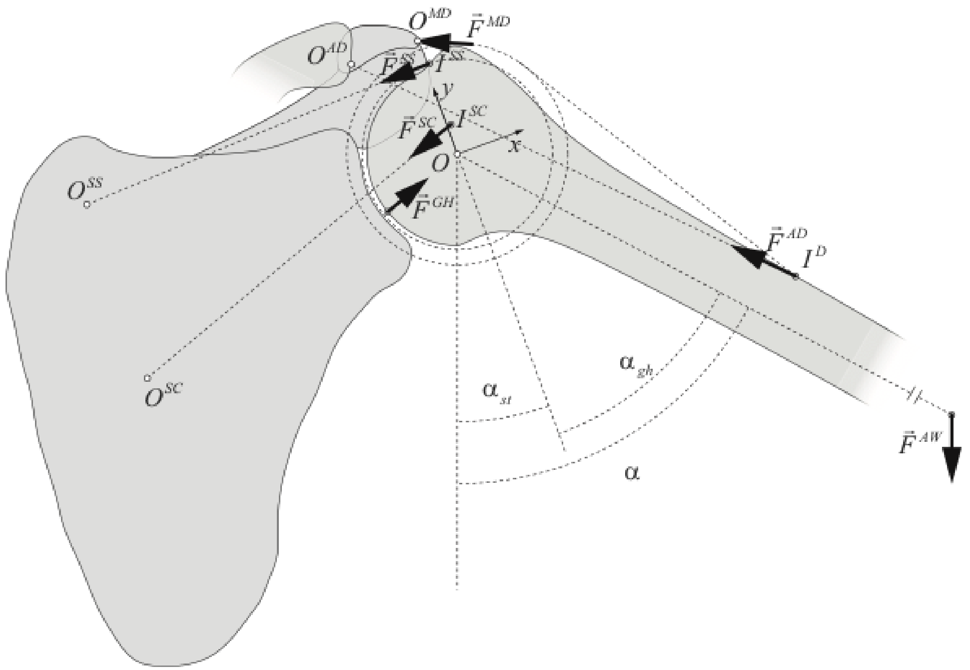

$$\alpha_{\mathrm{gh}} > \alpha_{\mathrm{gh}}^{\mathrm{MD_c}} = \sin^{-1}\left(\frac{R^{\mathrm{MD}}}{O^{\mathrm{MD}}}\right) - \sin^{-1}\left(\frac{O_x^{\mathrm{MD}}}{O^{\mathrm{MD}}}\right) + \sin^{-1}\left(\frac{R^{\mathrm{MD}}}{I^{\mathrm{MD}}}\right) - \sin^{-1}\left(\frac{I_X^{\mathrm{MD}}}{I^{\mathrm{MD}}}\right)$$

$$\alpha_{\mathrm{gh}} > \alpha_{\mathrm{gh}}^{\mathrm{SS_c}} = \sin^{-1}\left(\frac{R^{\mathrm{SS}}}{O^{\mathrm{SS}}}\right) - \sin^{-1}\left(\frac{O_y^{\mathrm{SS}}}{O^{\mathrm{SS}}}\right) + \sin^{-1}\left(\frac{R^{\mathrm{SS}}}{I^{\mathrm{SS}}}\right) - \sin^{-1}\left(\frac{I_Y^{\mathrm{SS}}}{I^{\mathrm{SS}}}\right)$$

$$F^{\mathrm{MD}} = F^{\mathrm{AW}} \frac{X^{\mathrm{AW}} \sin(\alpha)}{\sum_K r^K X^K \sin(\Delta\alpha^K)}$$

Parameter	Symbol	Value
Muscle origins [mm]		
Middle deltoid	$(O_x^{\mathrm{MD}}, O_y^{\mathrm{MD}})$	(2, 33)
Anterior deltoid	$(O_x^{\mathrm{AD}}, O_y^{\mathrm{AD}})$	(−15, 29)
Posterior deltoid	$(O_x^{\mathrm{PD}}, O_y^{\mathrm{PD}})$	(−55, 23)
Supraspinatus	$(O_x^{\mathrm{SS}}, O_y^{\mathrm{SS}})$	(−81, 25)
Subscapularis	$(O_x^{\mathrm{SC}}, O_y^{\mathrm{SC}})$	(−99, −23)
Infraspinatus	$(O_x^{\mathrm{IS}}, O_y^{\mathrm{IS}})$	(−97, −22)
Muscle insertions [mm]		
Middle deltoid	$(I_{x0}^{\mathrm{MD}}, I_{y0}^{\mathrm{MD}})$	(20, −90)
Anterior deltoid	$(I_{x0}^{\mathrm{AD}}, I_{y0}^{\mathrm{AD}})$	(20, −90)
Posterior deltoid	$(I_{y0}^{\mathrm{PD}}, I_{y0}^{\mathrm{PD}})$	(20, −90)
Supraspinatus	$(I_{x0}^{\mathrm{SS}}, I_{x0}^{\mathrm{SS}})$	(23, 13)
Subscapularis	$(I_{y0}^{\mathrm{SC}}, I_{x0}^{\mathrm{SC}})$	(0, 10)
Infraspinatus	$(I_{x0}^{\mathrm{IS}}, I_{y0}^{\mathrm{IS}})$	(5, 9)
Muscle ratios		
Middle deltoid	r^{MD}	1.0
Anterior deltoid	r^{AD}	0.8
Posterior deltoid	r^{PD}	0.2
Supraspinatus	r^{SS}	0.5
Subscapularis	r^{SC}	0.5
Infraspinatus	r^{IS}	0.5
Contact radii [mm]		
Middle deltoid	R^{MD}	30
Supraspinatus	R^{SS}	26
Arm gravity centre [mm]		
X^{A}	320	
Arm mass [kg]		
M^{A}	3.75	
Scapulohumeral rhythm		
r_{sh}	2	
Gravity constant [m/s^2]		
g	10	

2D numerical model

- Theoretically identical to algebraic model
- Conceptually different from algebraic model
- Movement not fully known (**humerus translations**)
- Nonlinear equations solved iteratively
- Problem: muscles synchronization
- Solution:
  - Set deltoid medium shortening
  - Get deltoid medium force
  - Synchronize force of other muscles

2D numerical model

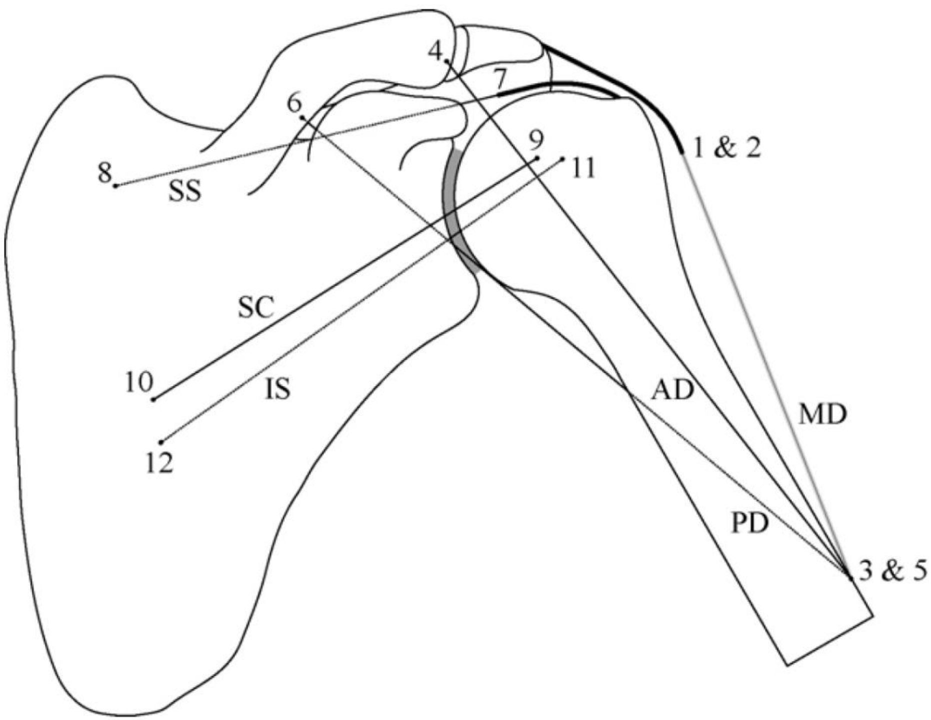

$$K^{NM} = -\frac{dF^{N}}{du^{M}}$$

- Joint contact (humerus migration)
- Muscle wrapping (stability)
- Muscle force synchronization
- Feedback algorithm
- Development of a new element (FEM)
- Algebraic form of the Jacobian K
- Guarantee muscle activation ratios
- Satisfy mechanical equilibrium

2D numerical model

Stabilizing effect of rotator cuff muscles

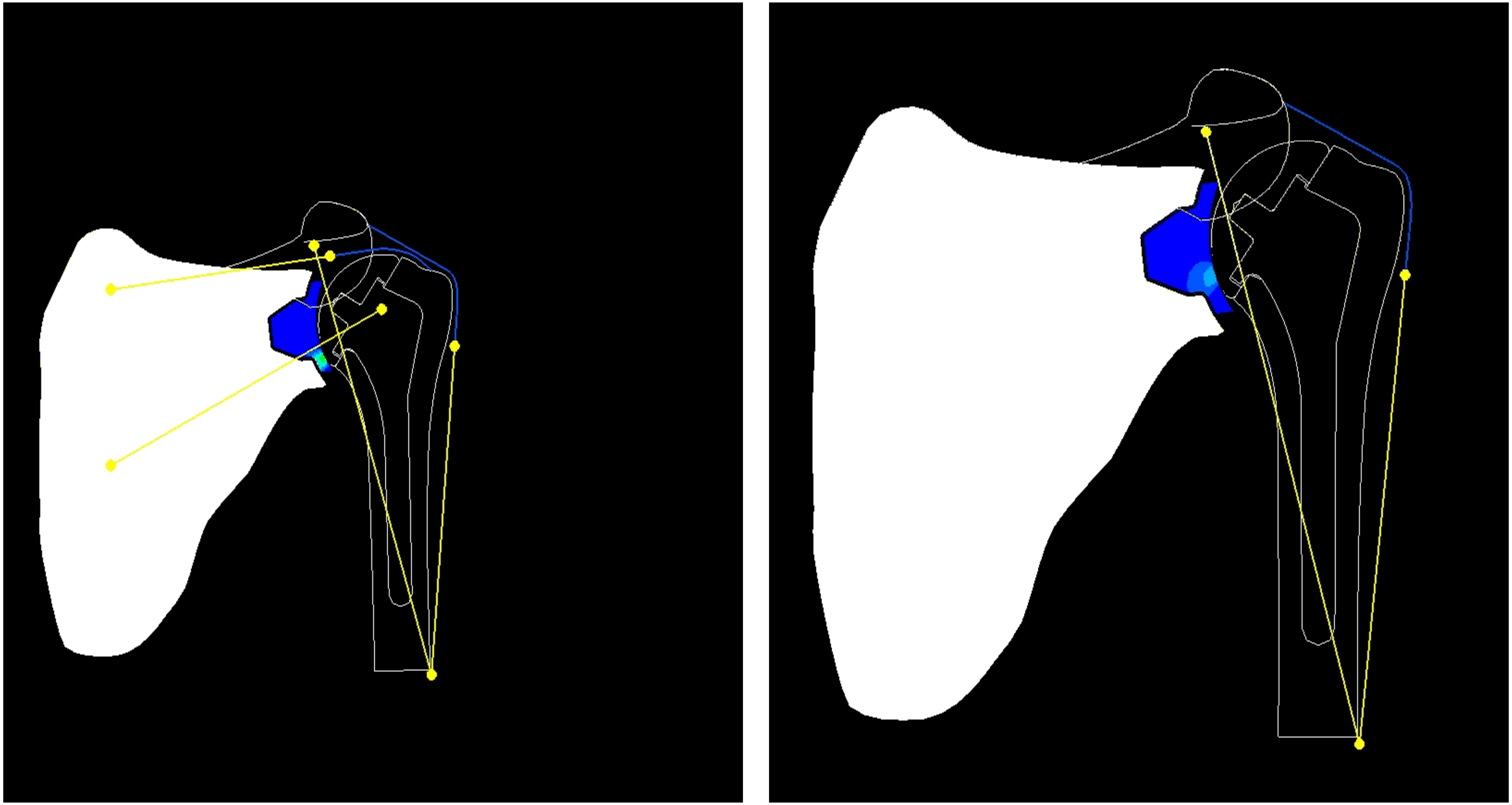

3D numerical model

- CT: Geometry + local bone properties
- Dissection: muscles insertions
- Arthroplasty with CAD

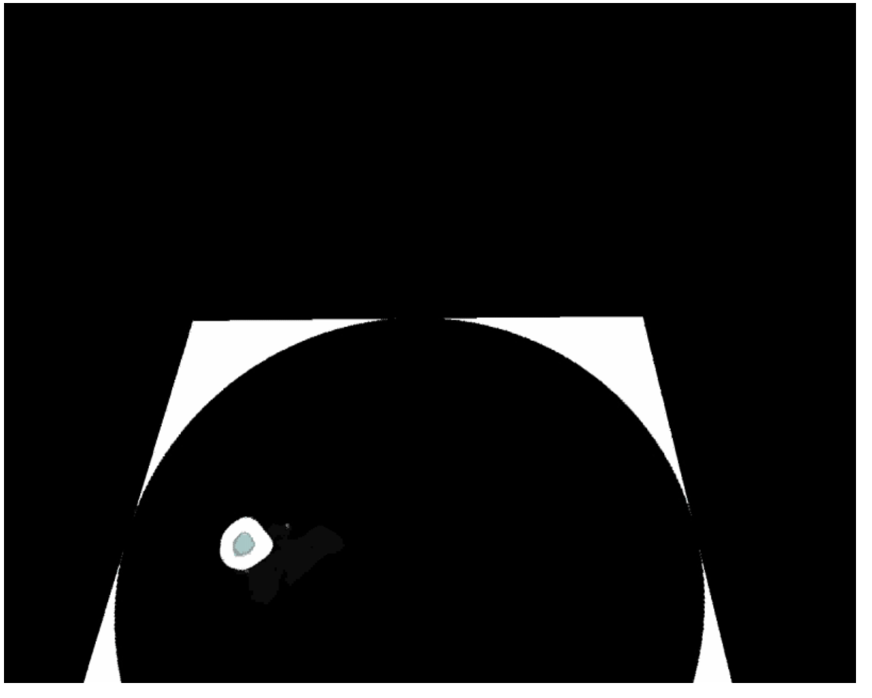

Shoulder

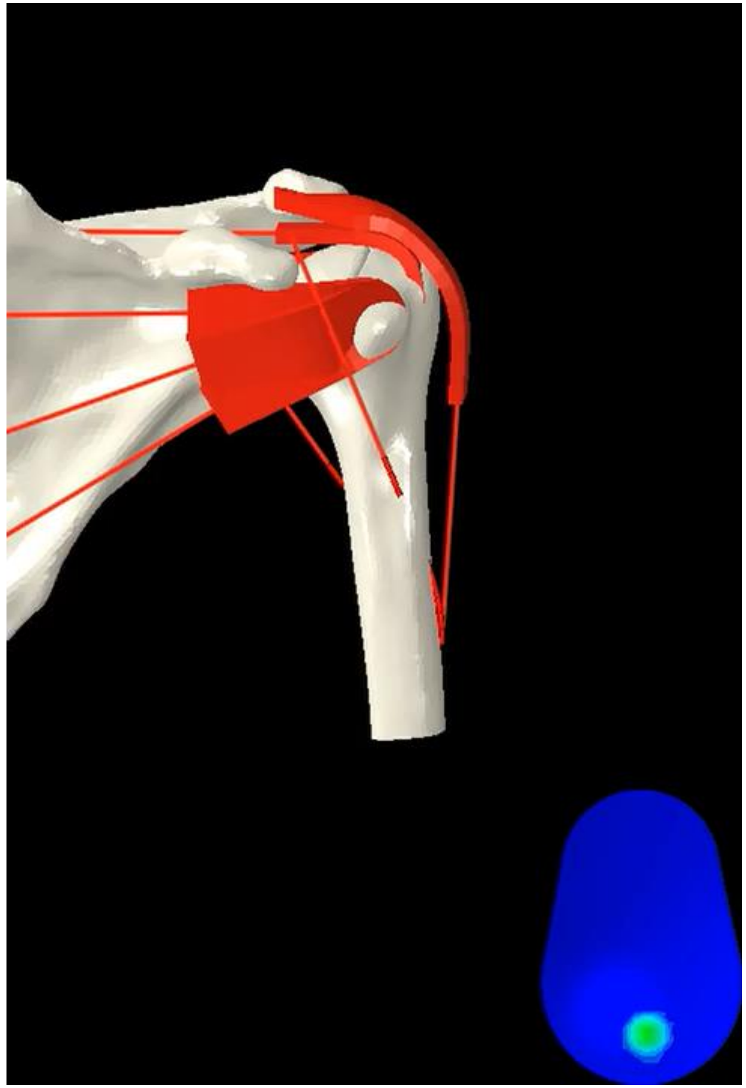

EPFL-LBO (A. Terrier)

Verification

Comparison to the algebraic solution

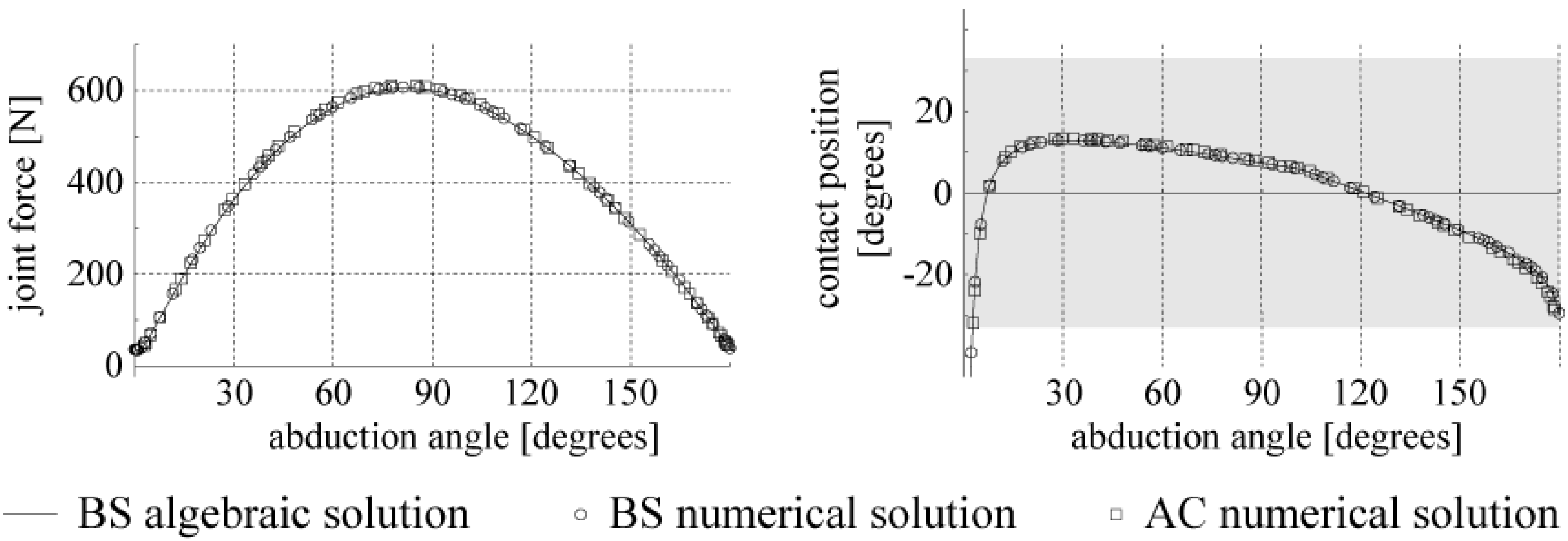

Compare with Poppen & Walker

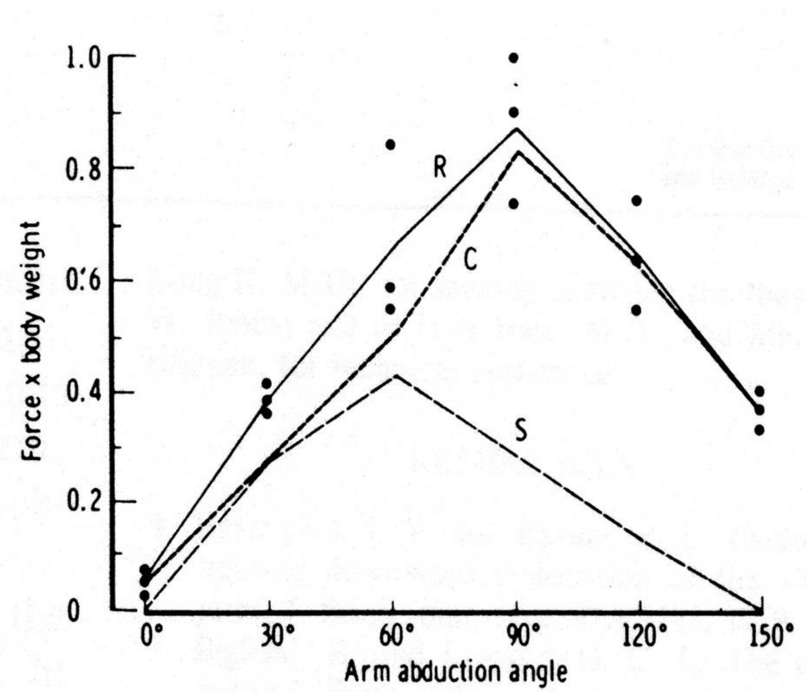

Poppen & Walker (1978)

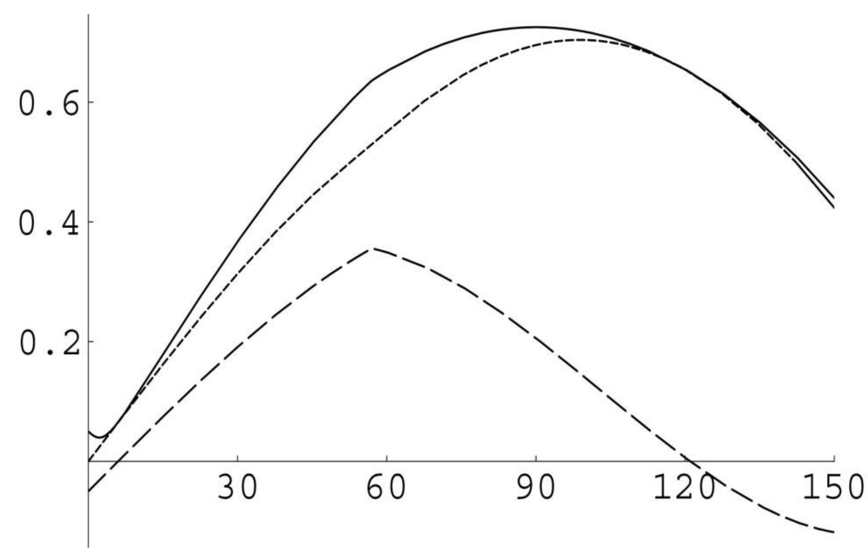

Terrier, 2006

Compare with van der Helm

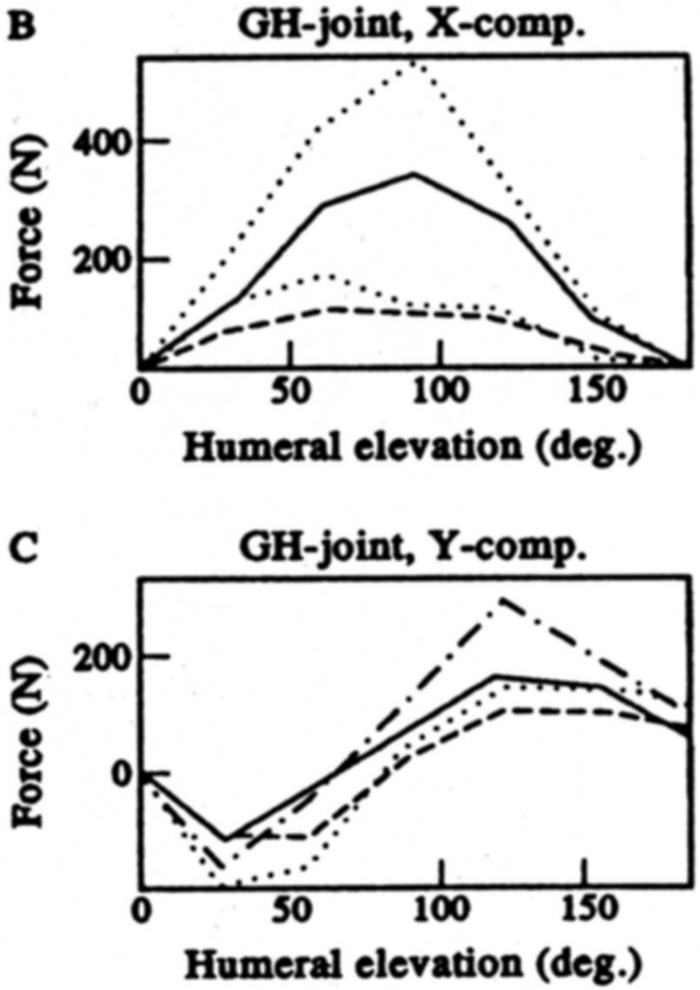

Van der Helm, 1994

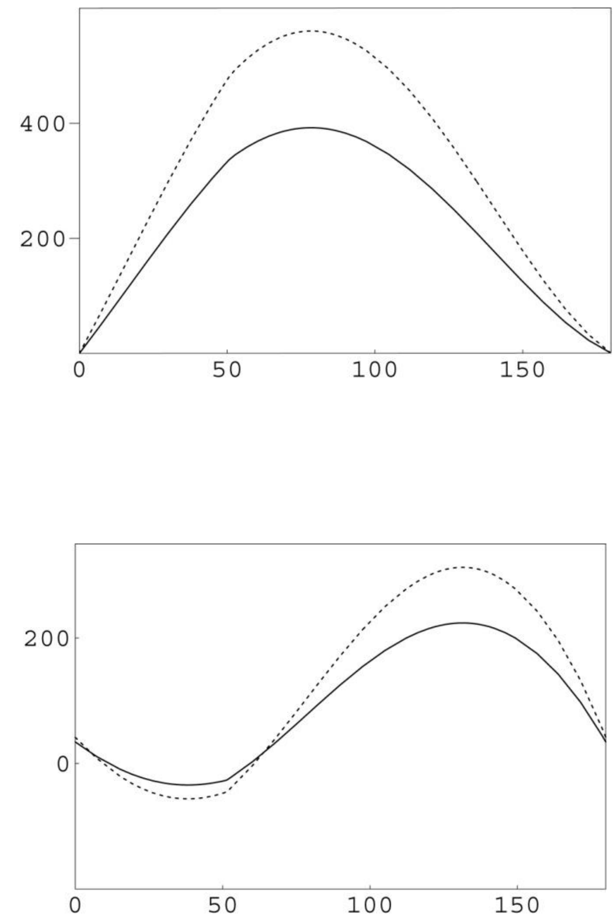

Terrier, 2006

Humerus translation

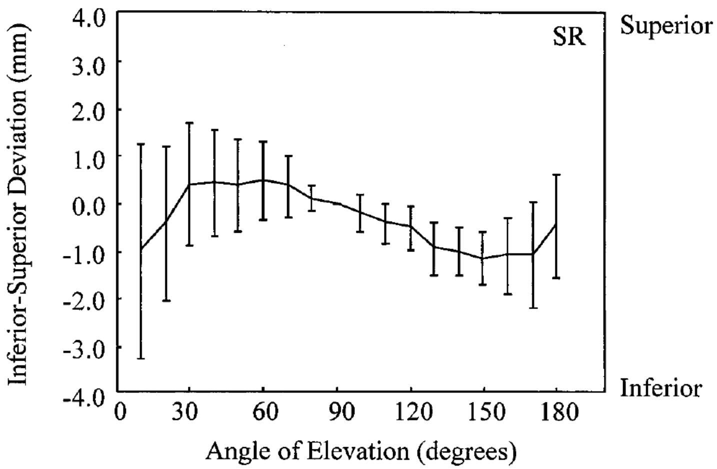

Kelkar et al, JSES, 2001

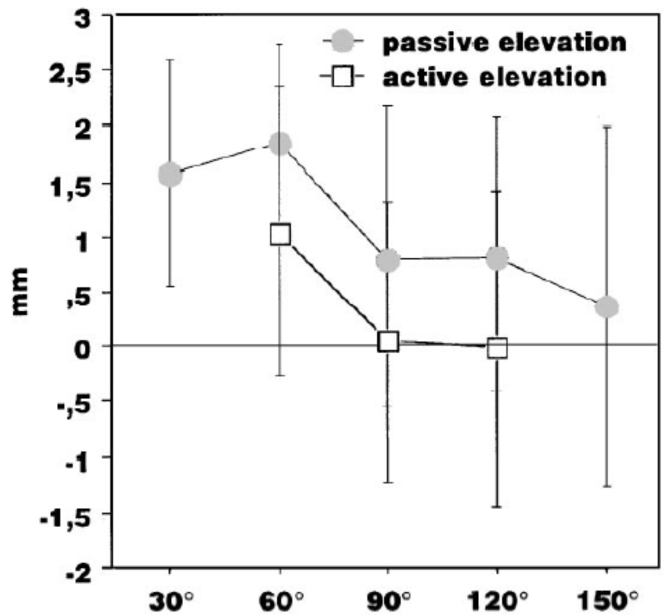

Graichen et al, JB 2000

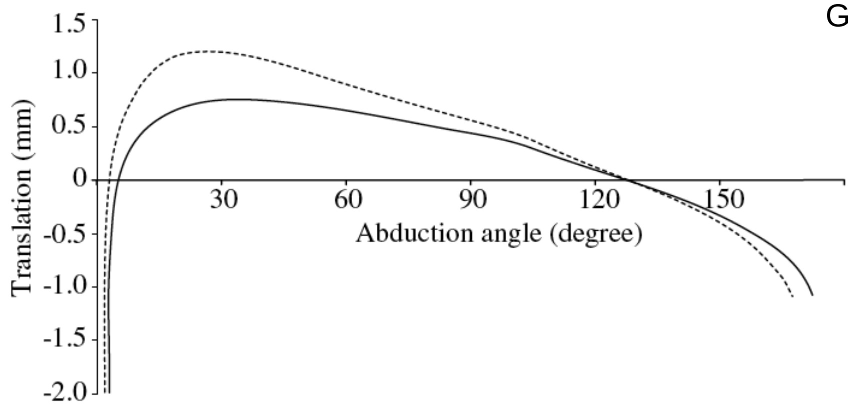

Terrier et al, 2007

Joint contact pattern

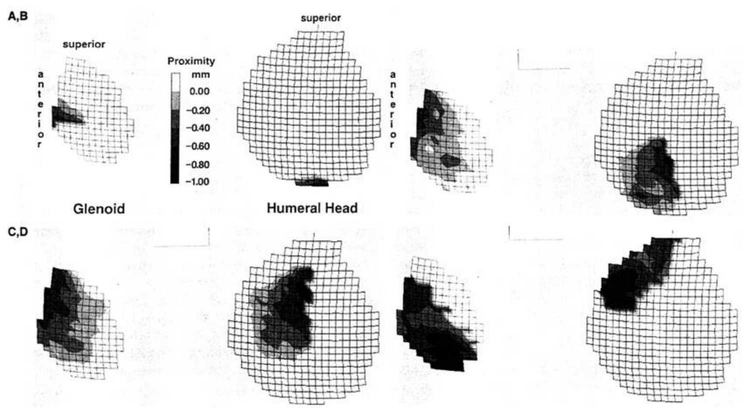

FIG. 6. Glenohumeral contact patterns for a typical shoulder at (A) 0°, (B) 60°, (C) 120°, and (D) 180° of elevation in the scapular plane in the starting rotation (SR) and at (E) 0°, (F) 60°, (G) 120°, and (H) 180° of elevation in the scapular plane 20° internally rotated to the (SR). Gray levels are proportional to the degree of overlap of the articular surfaces. Dramatic shifts in contact are evident.

Soslowsky et al, 1992

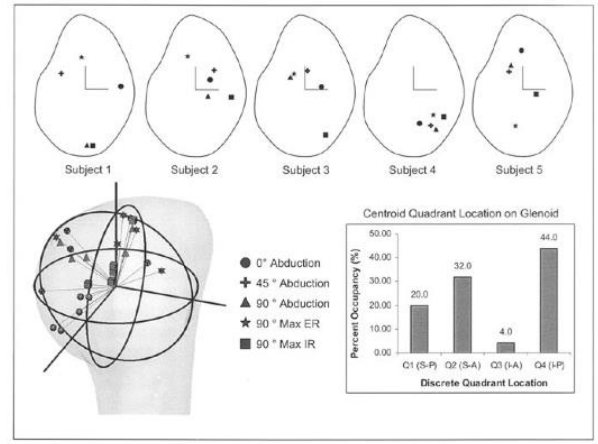

Boyer et al, 2008

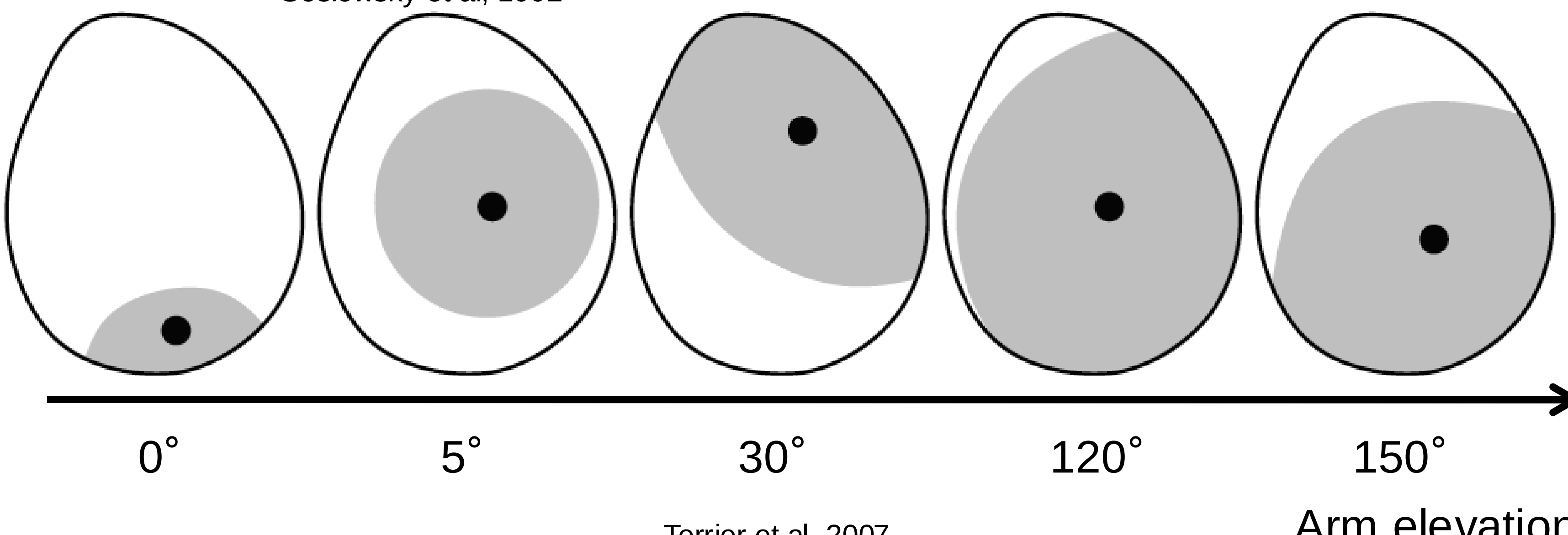

Terrier et al, 2007

Clinical application

Comparison of 2 prostheses

Clinical background

Anatomic prosthesis

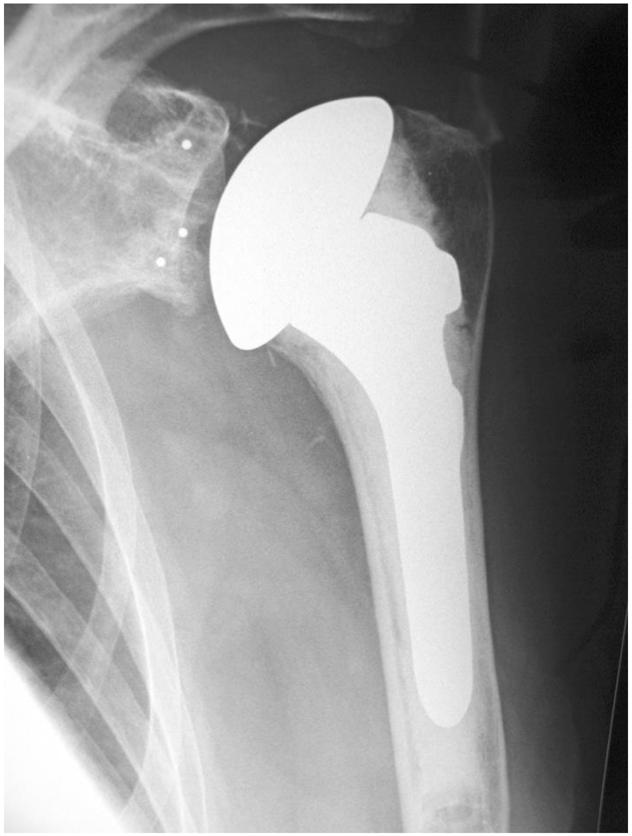

Reversed prosthesis

Clinical background

Anatomic prosthesis

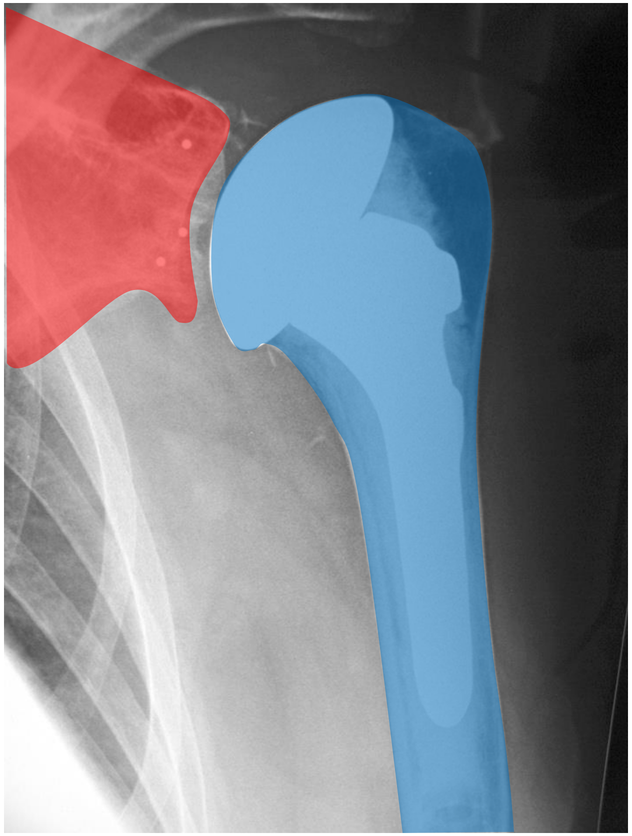

Reversed prosthesis

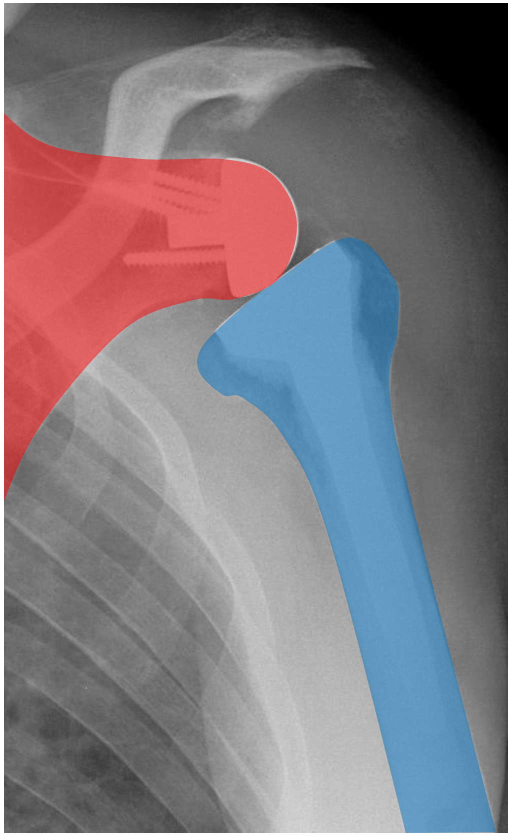

Clinical background

Anatomic prosthesis

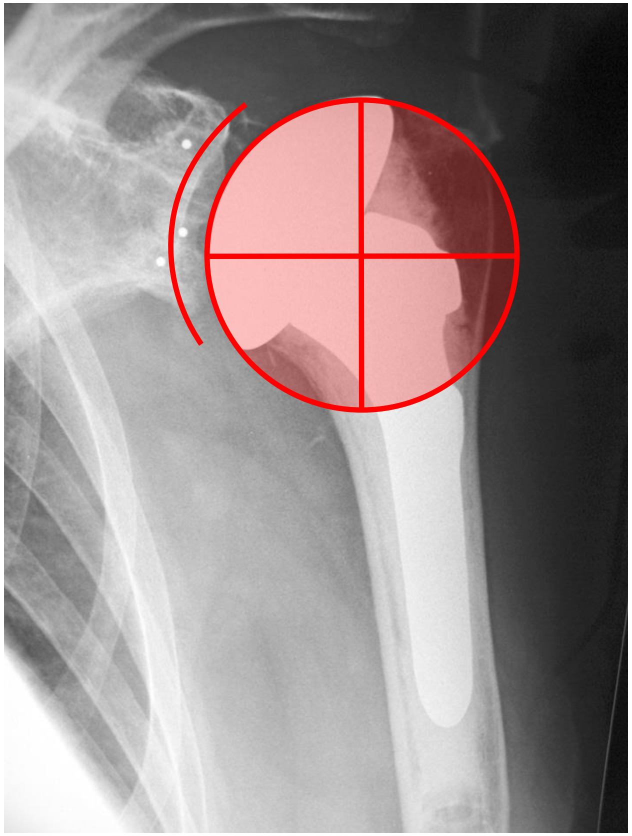

Reversed prosthesis

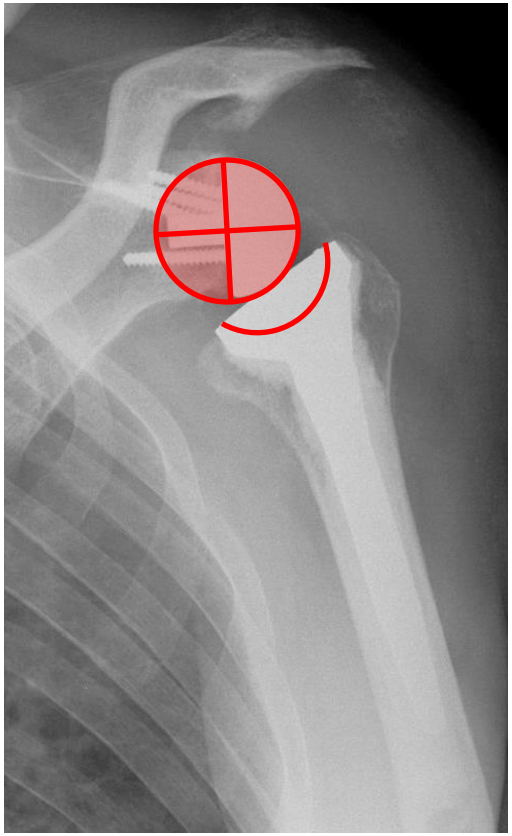

Clinical background

Anatomic prosthesis

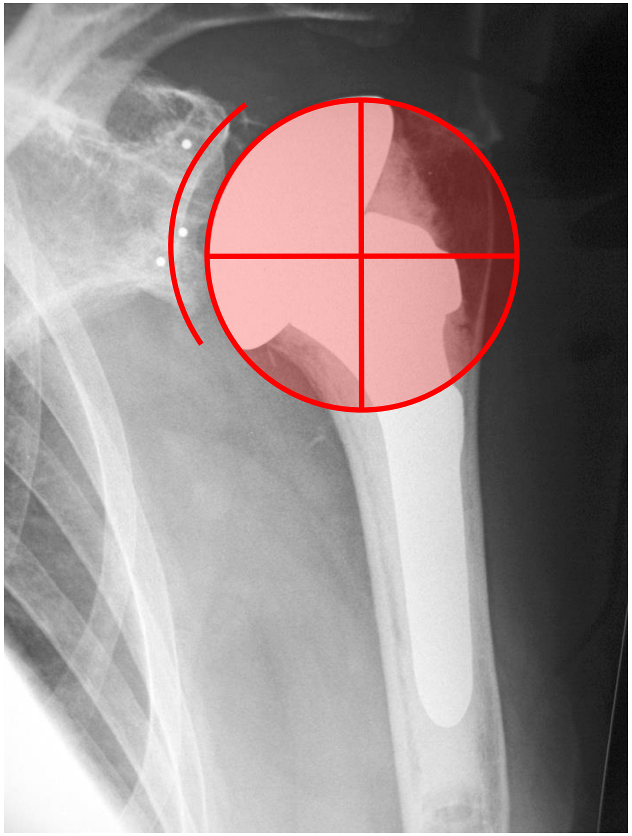

Reversed prosthesis

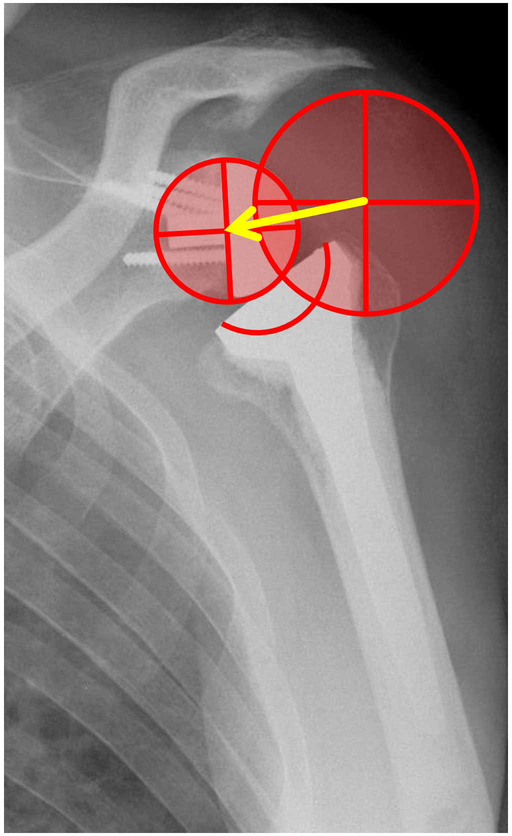

Clinical background

Anatomic prosthesis

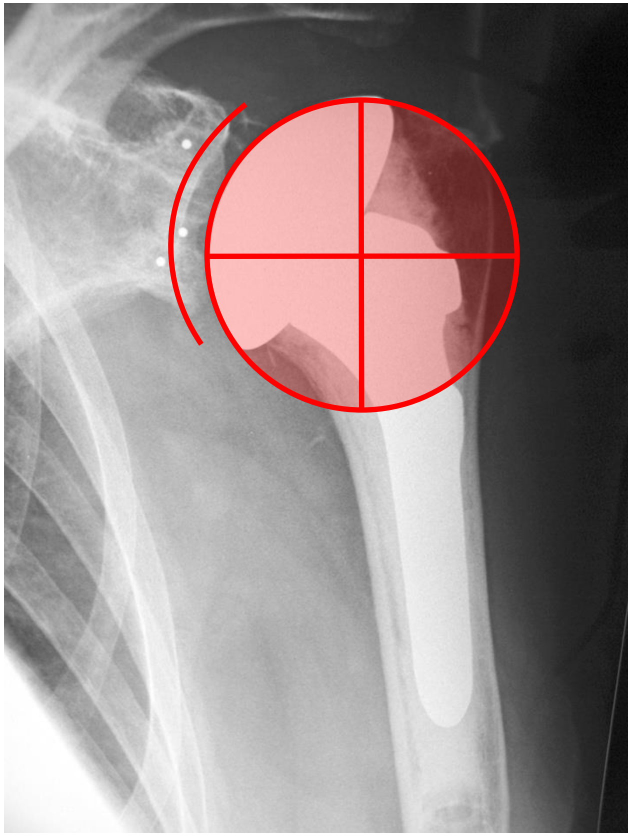

Reversed prosthesis

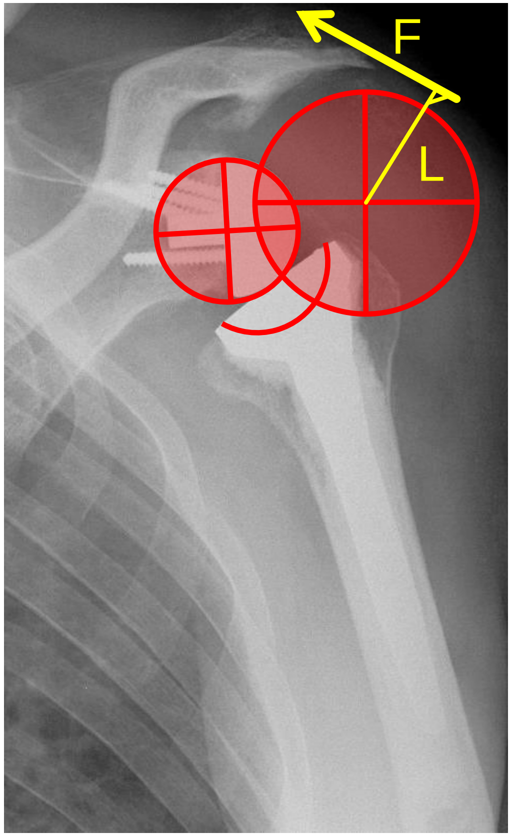

Clinical background

Anatomic prosthesis

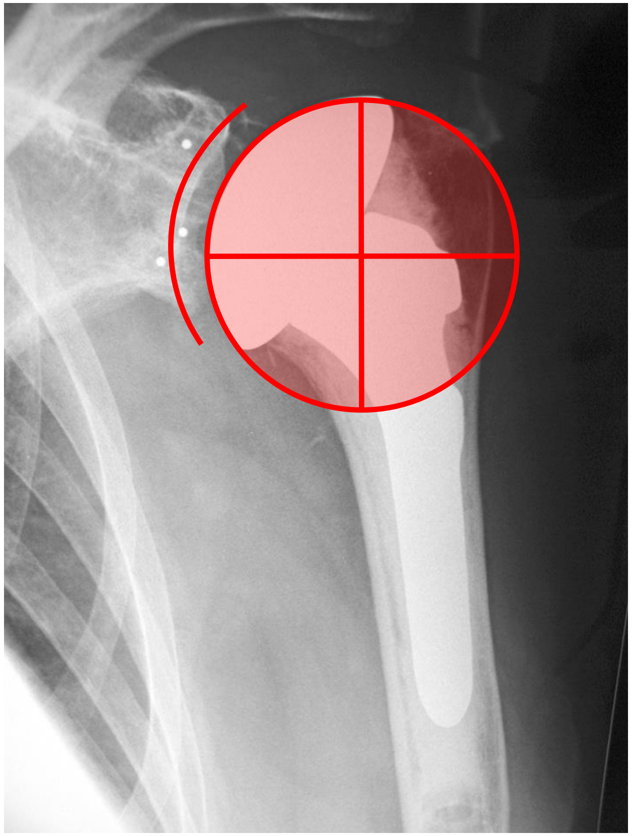

Reversed prosthesis

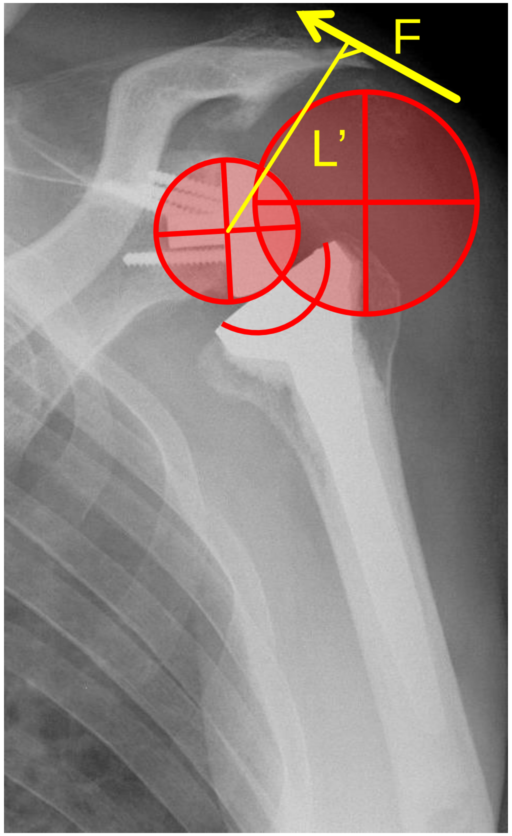

Clinical background

Anatomic prosthesis

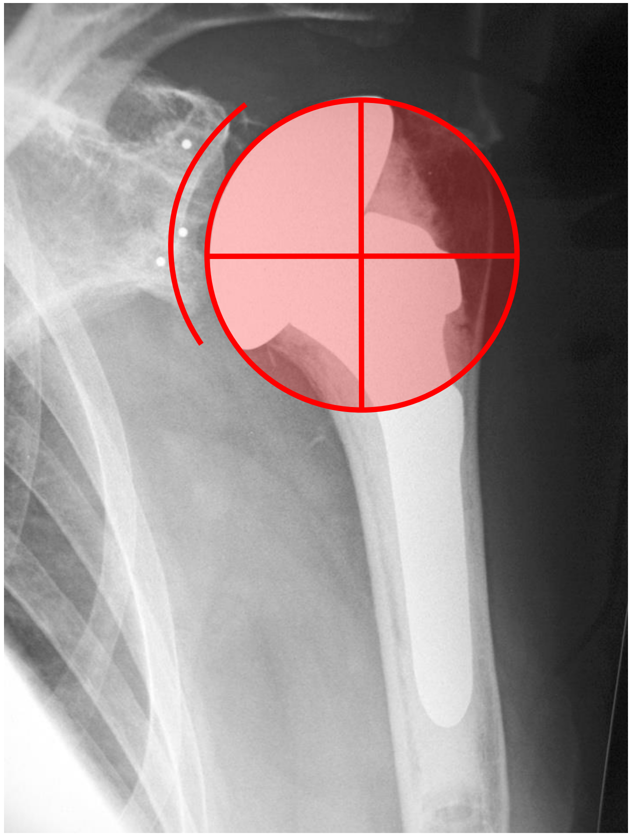

Reversed prosthesis

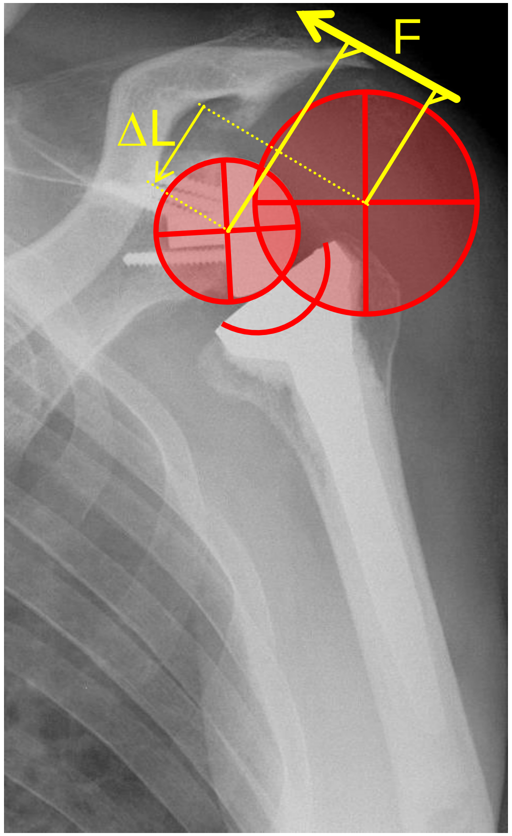

Clinical question

Functional muscles

↓

Anatomic prosthesis

↓

Polyethylene wear !

Deficient muscles

↓

Reversed prosthesis

↓

Polyethylene wear ?

(follow-up)

Preliminary answer

Predict polyethylene wear

on a reversed prosthesis

and compare to

an anatomic prosthesis

Method: numerical model

Anatomic prosthesis

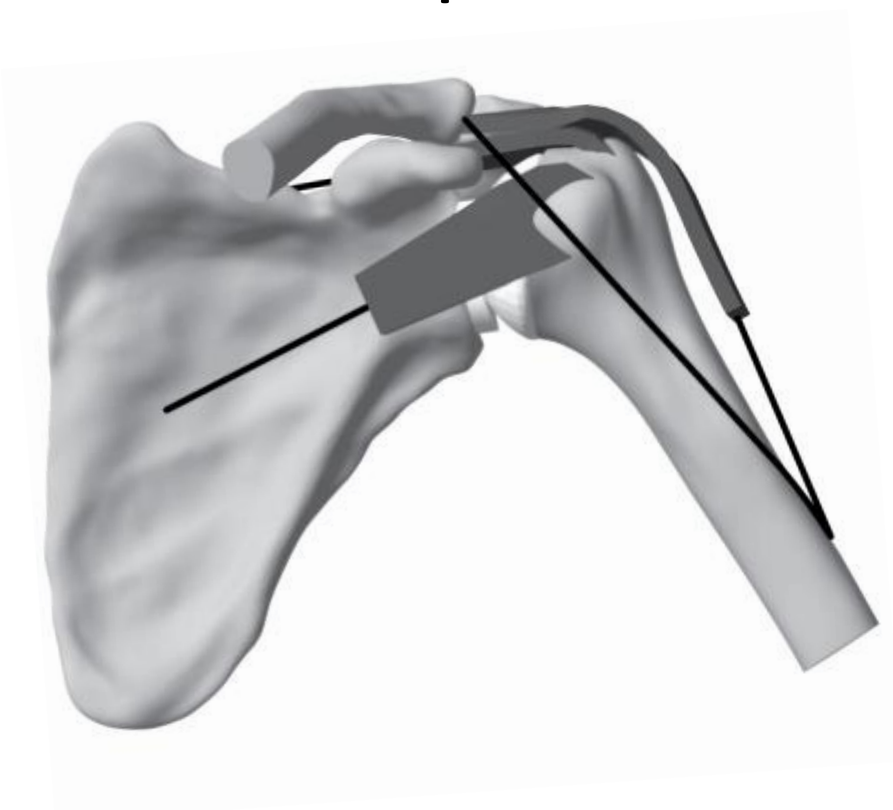

Reversed prosthesis

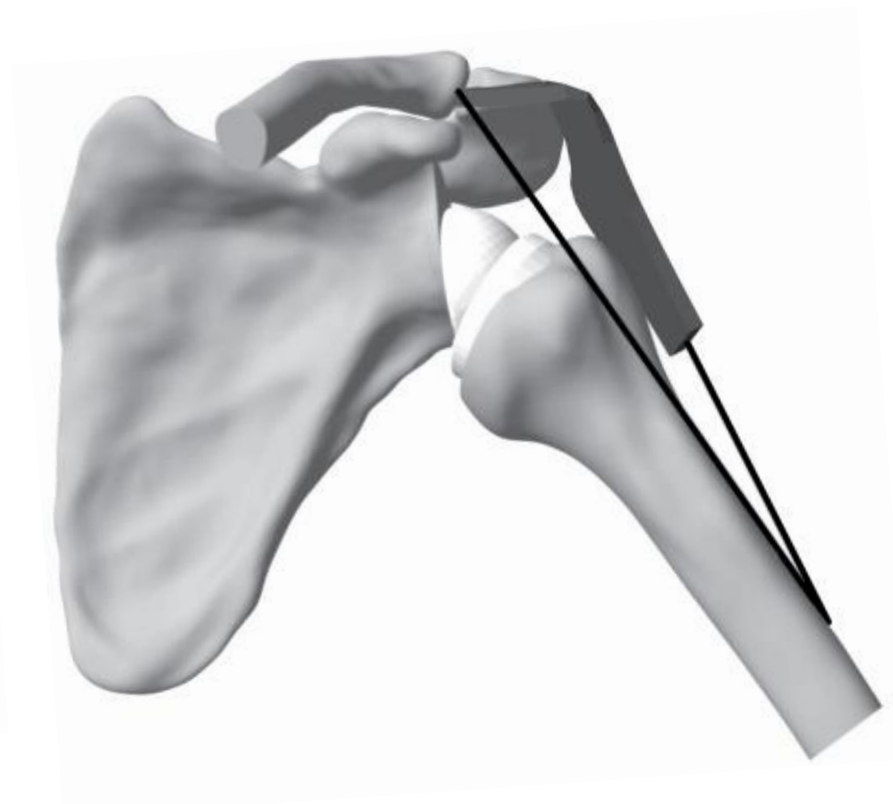

Method: numerical model

Anatomic prosthesis

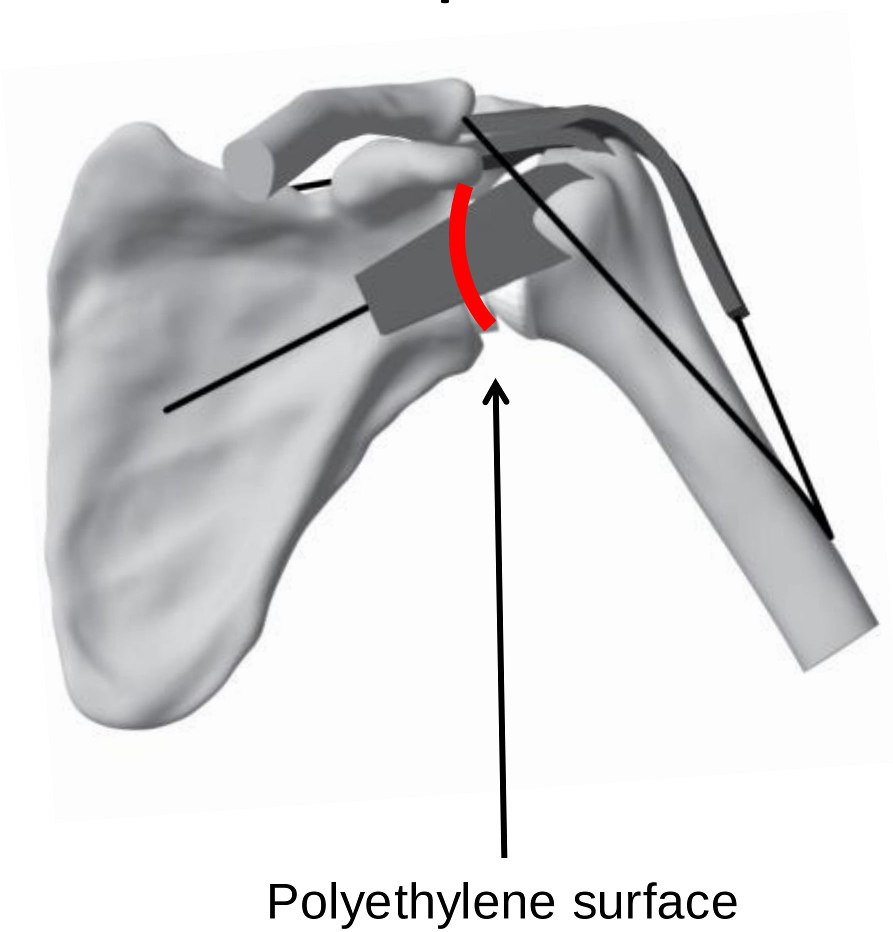

Reversed prosthesis

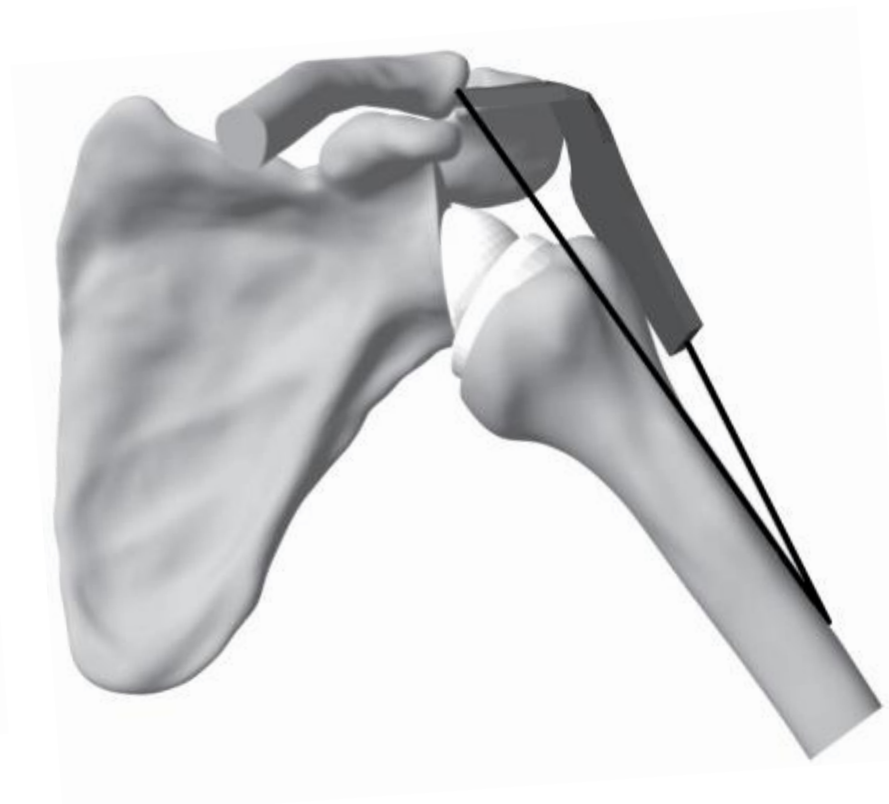

Method: numerical model

Anatomic prosthesis

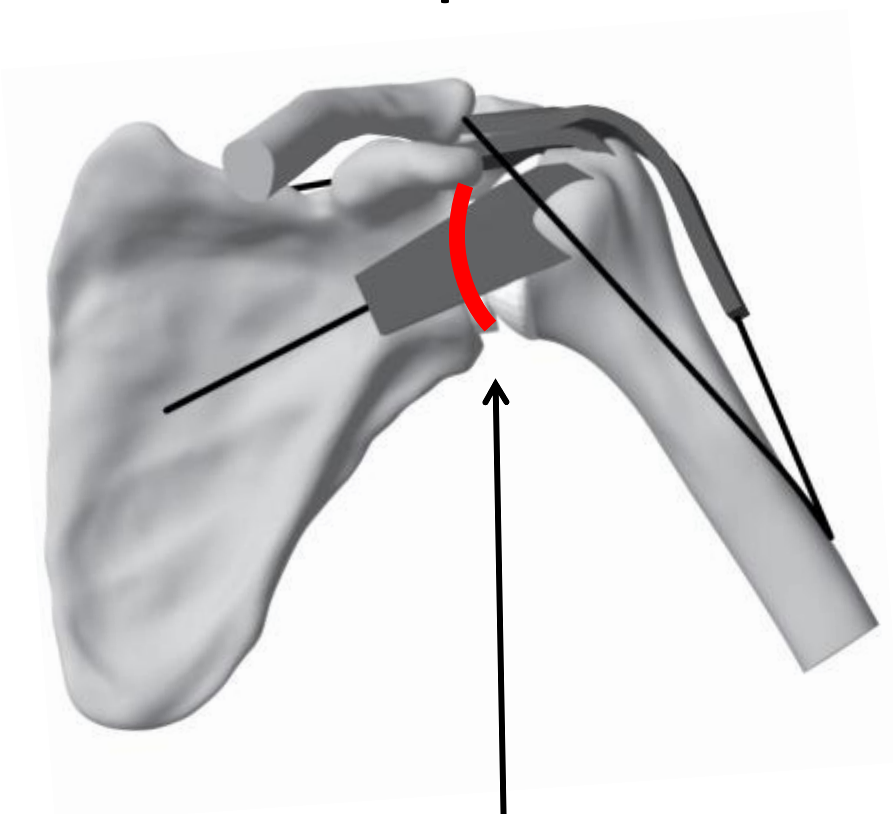

Polyethylene surface

Reversed prosthesis

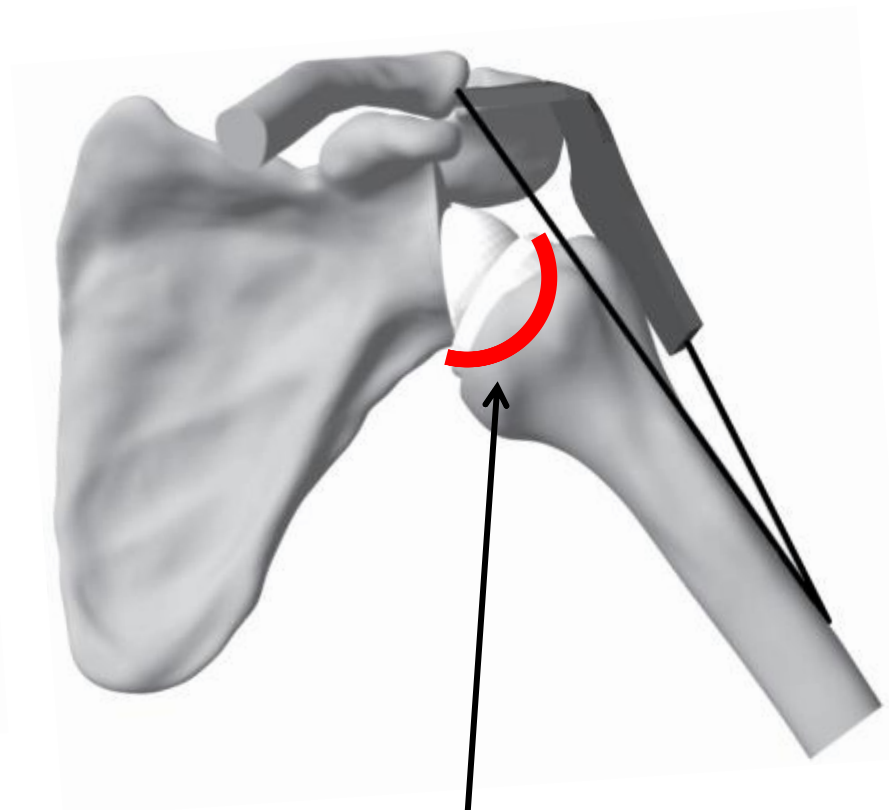

Polyethylene surface

Results: moment arms

Anatomic **Reversed**

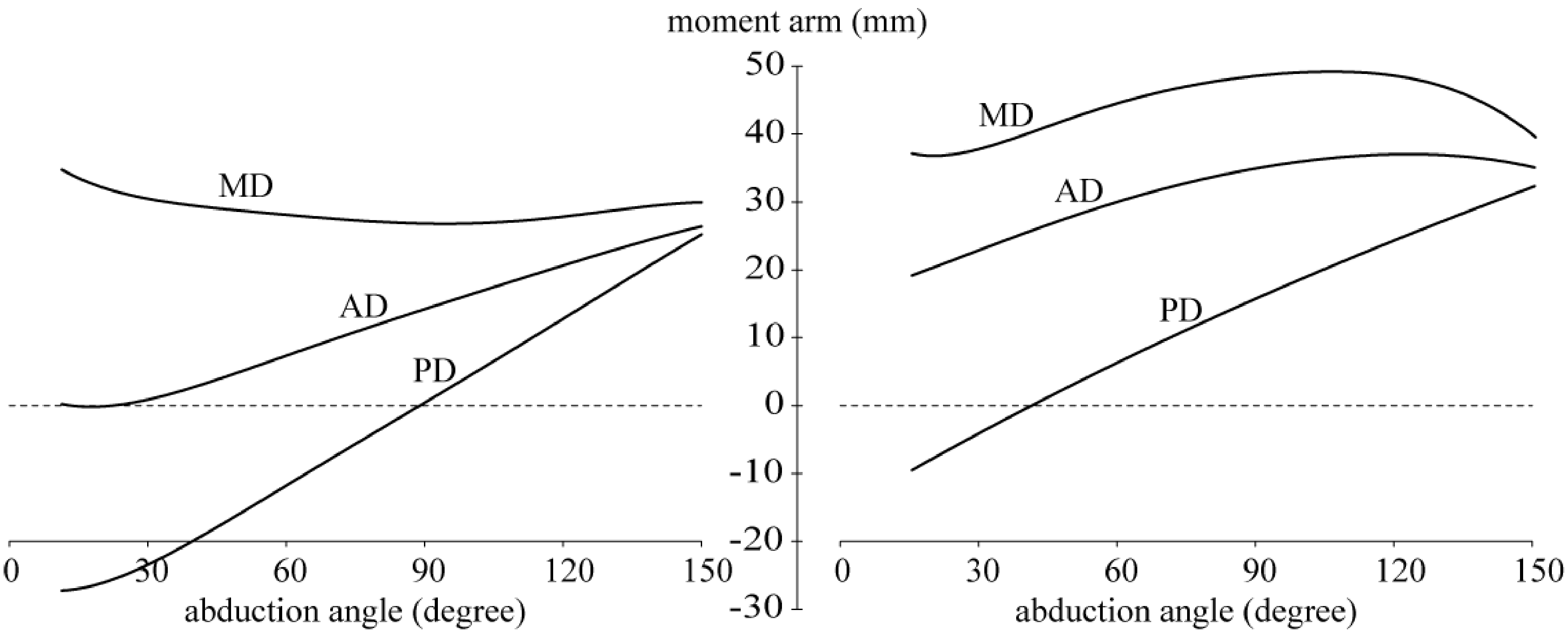

Results: moment arms

Anatomic **Reversed**

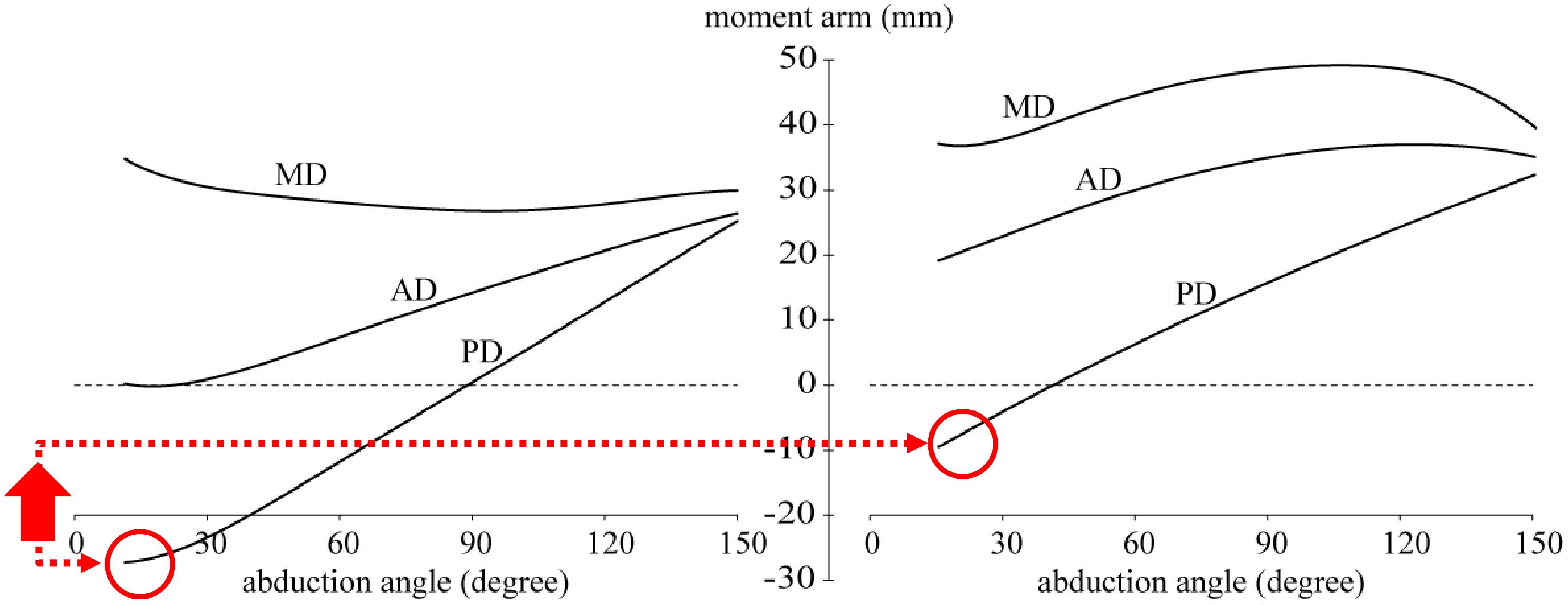

Results: moment arms

Anatomic | **Reversed**

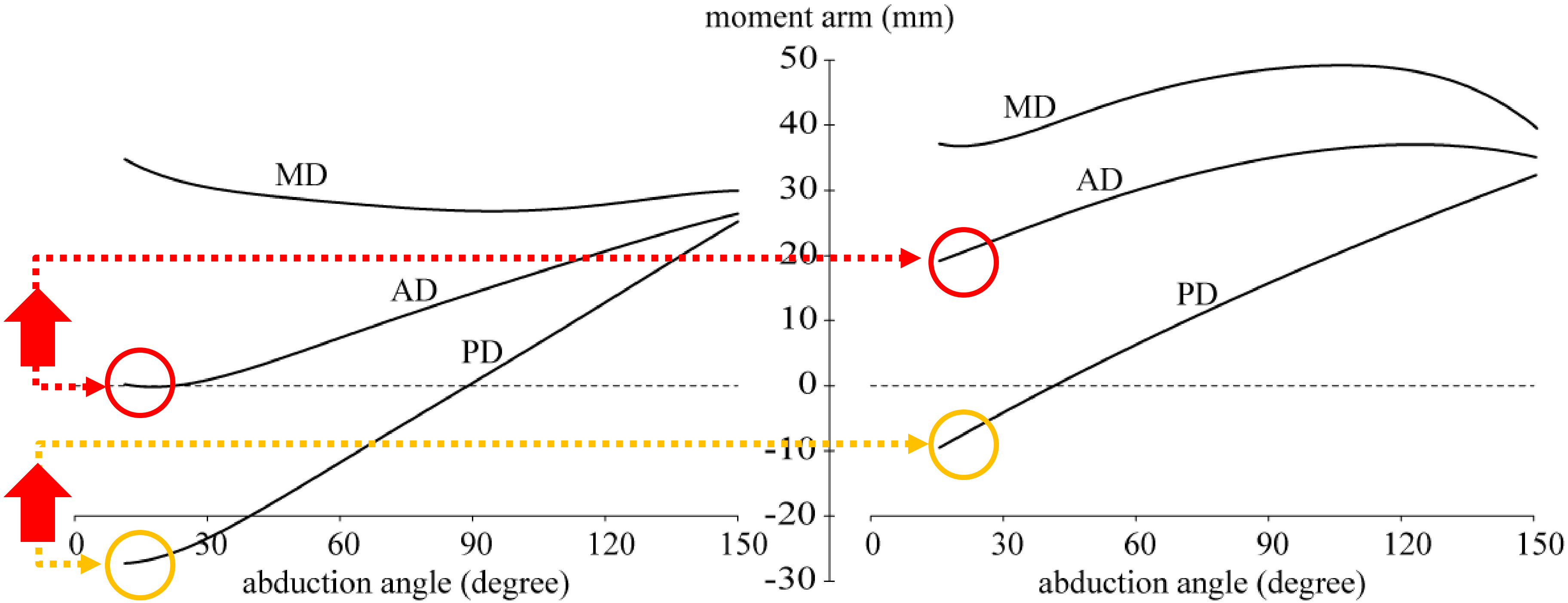

Results: moment arms

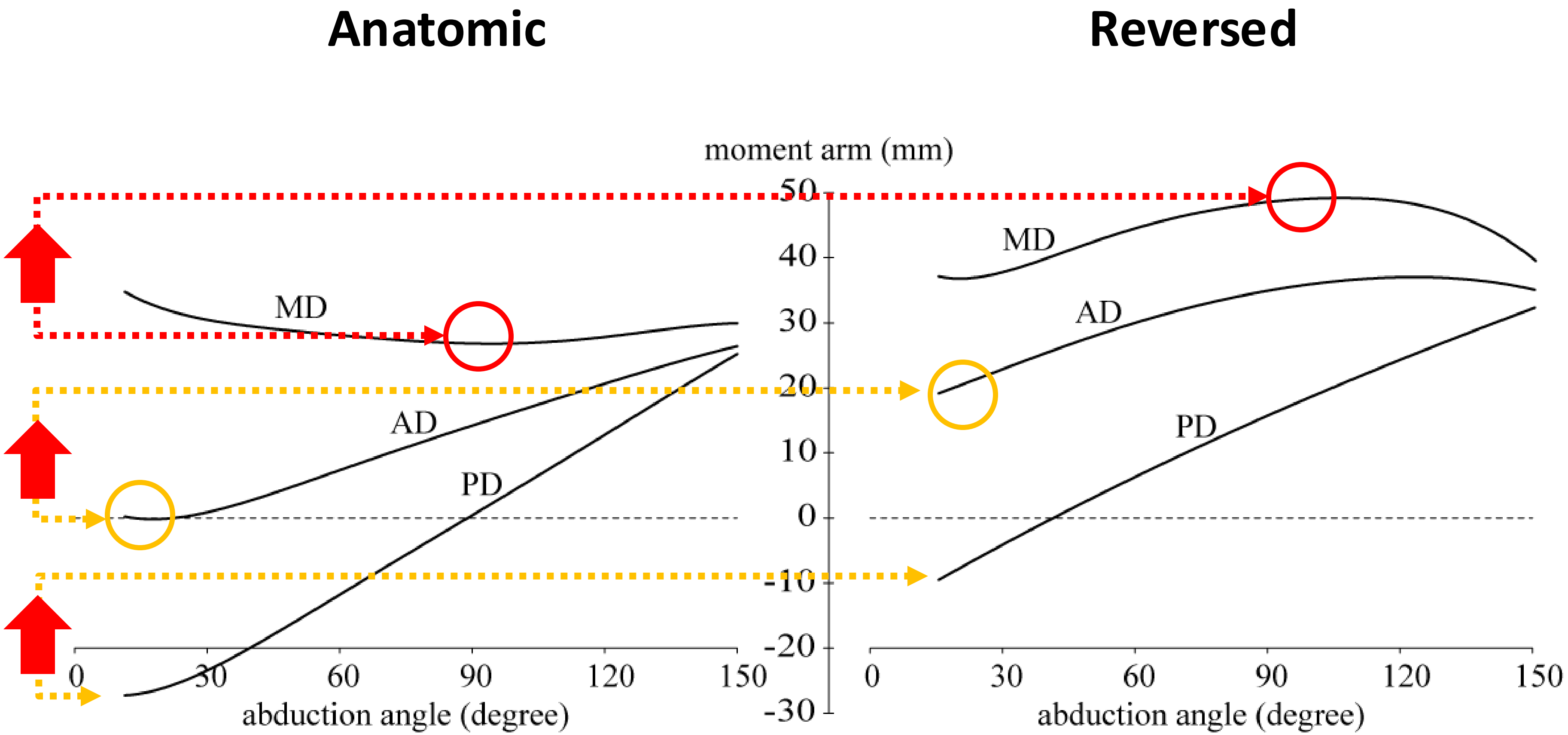

Results: joint & muscle forces

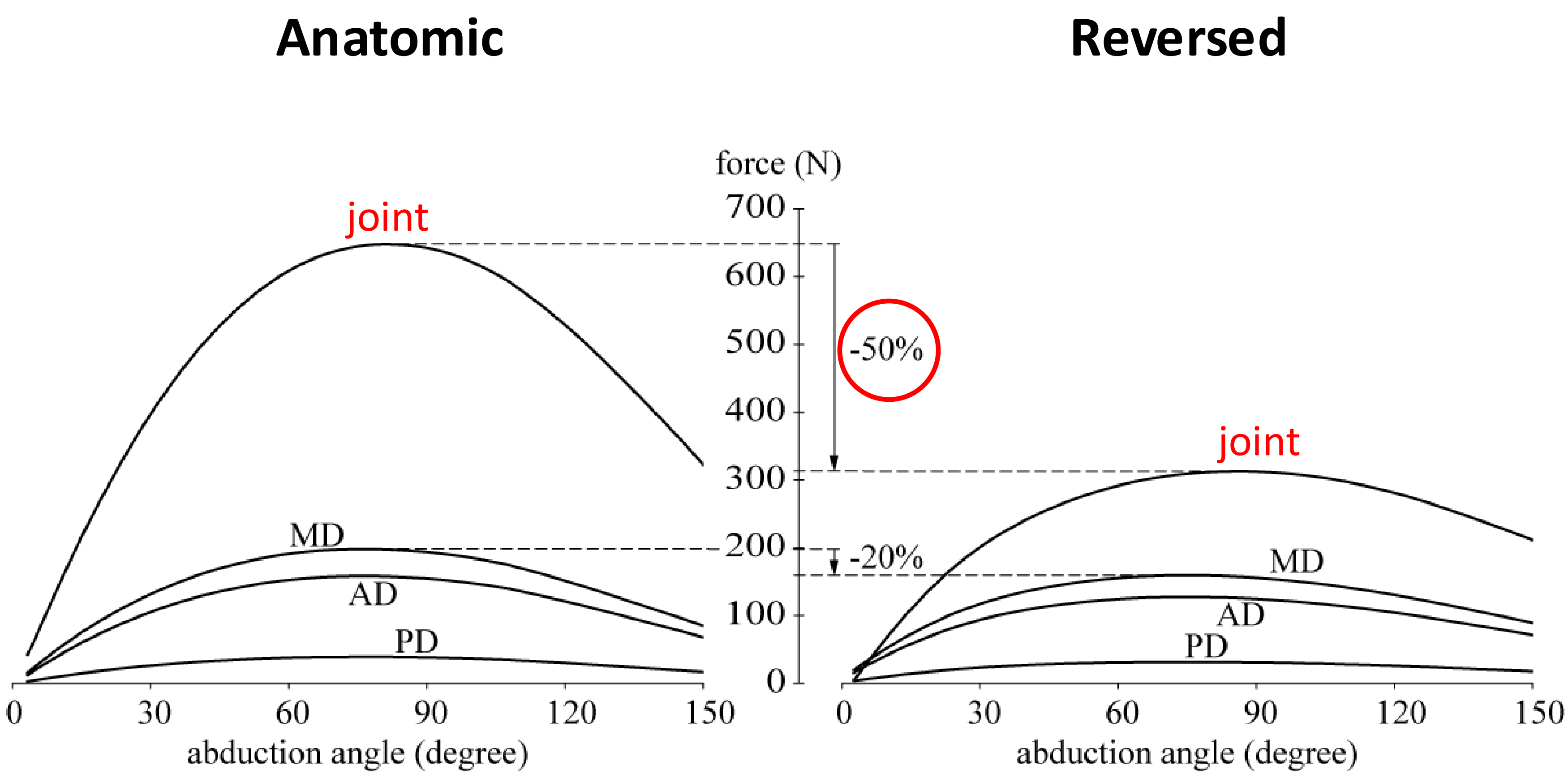

Results: Joint force

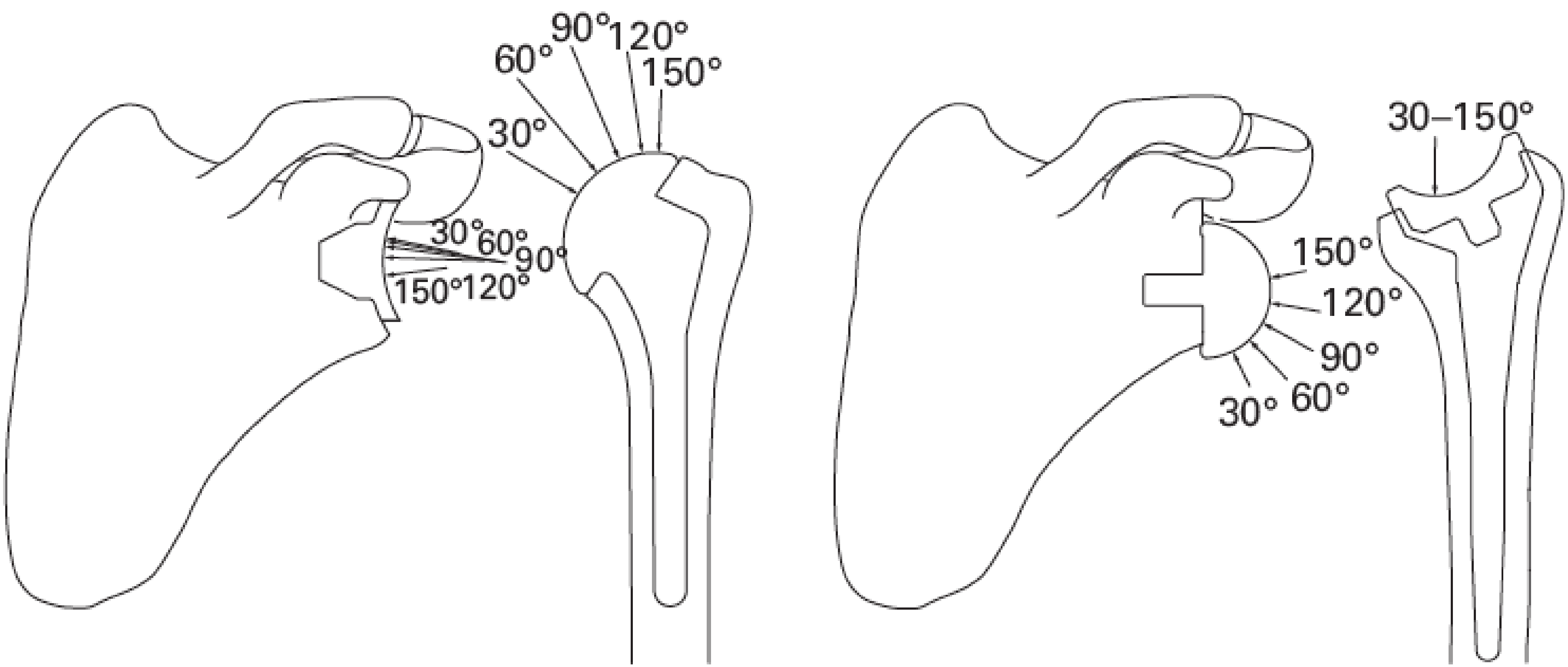

Results: contact pressure

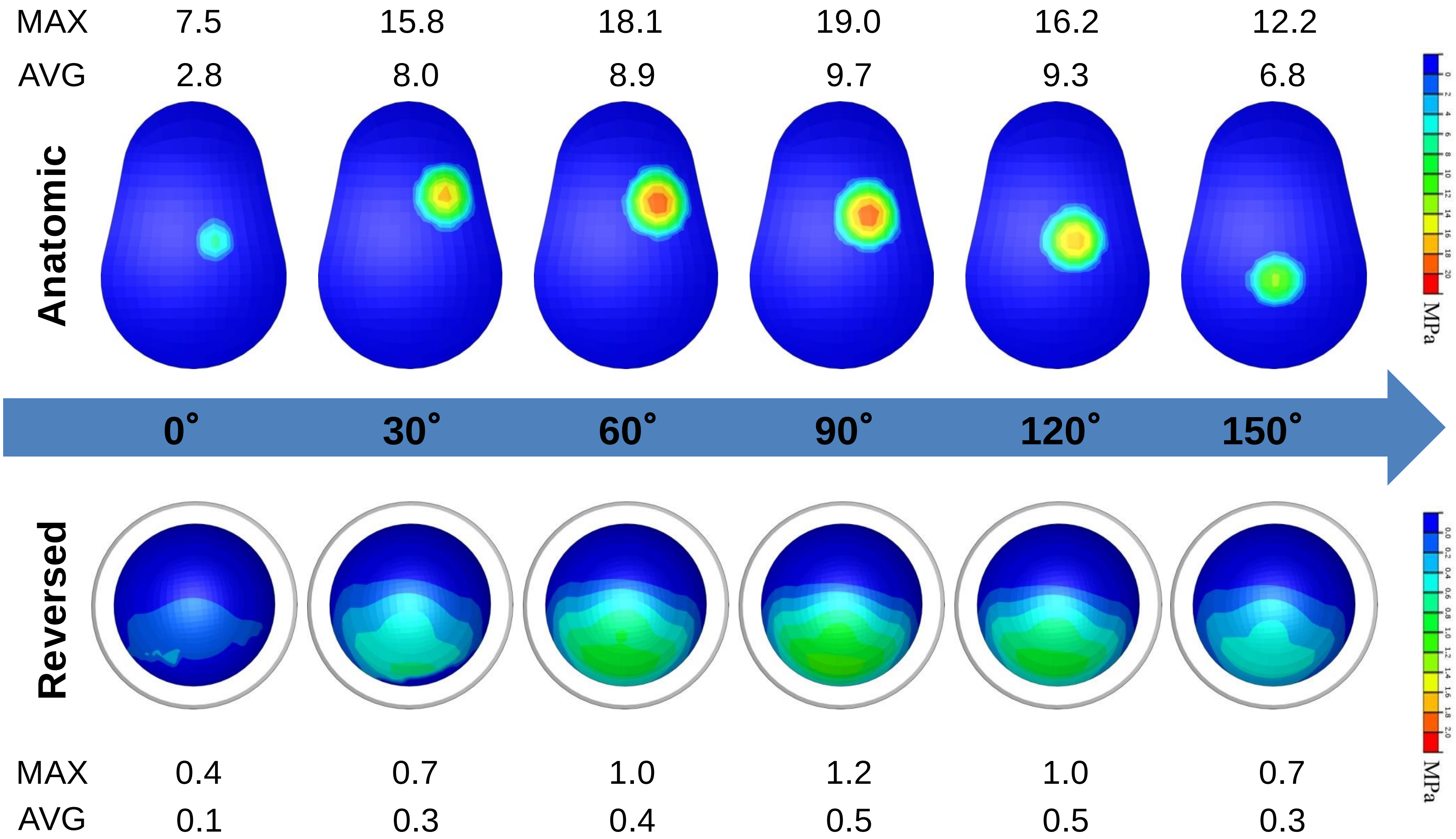

Results: contact pressure

MAX	7.5	15.8	18.1	19.0	16.2	12.2
AVG	2.8	8.0	8.9	9.7	9.3	6.8

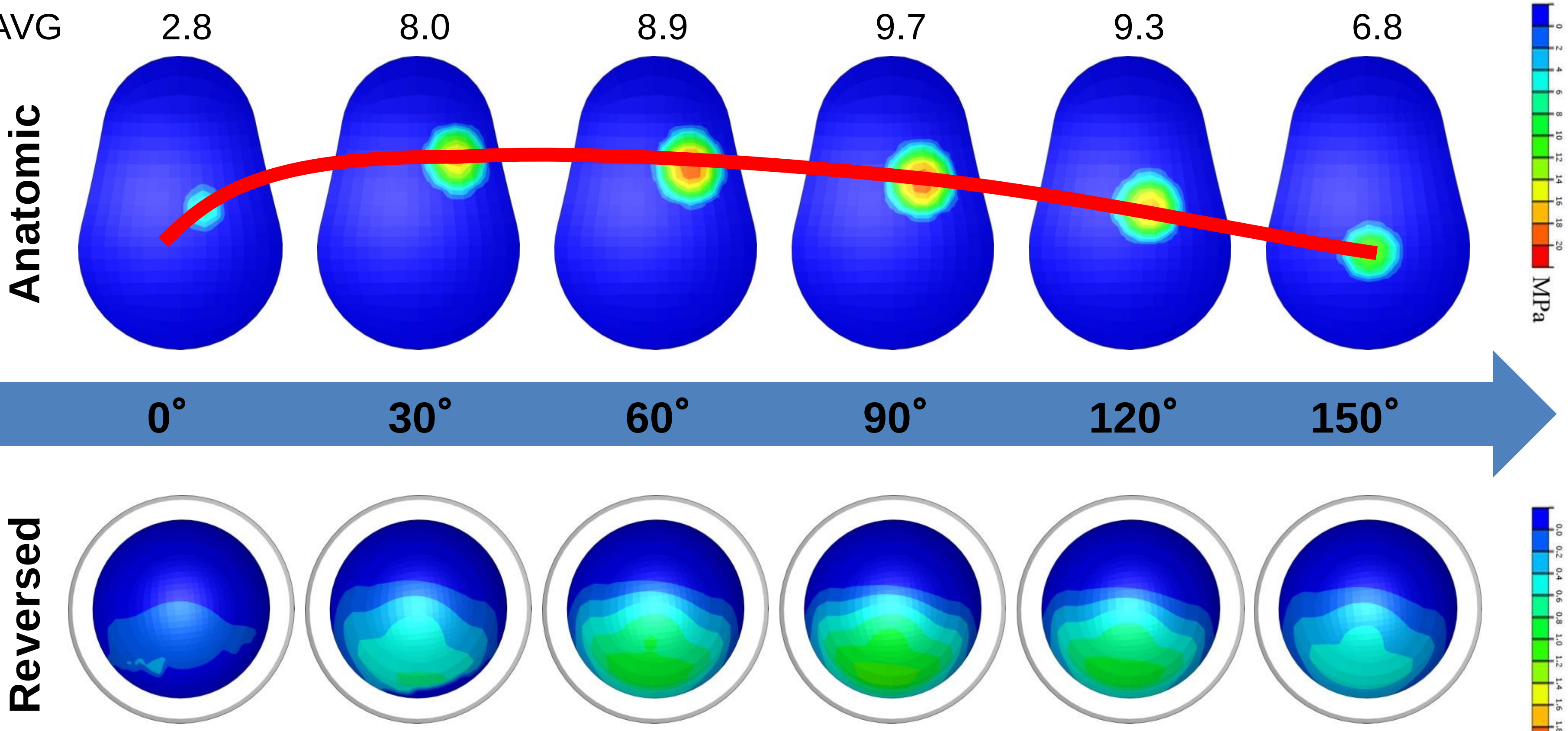

MAX	0.4	0.7	1.0	1.2	1.0	0.7
AVG	0.1	0.3	0.4	0.5	0.5	0.3

Results: contact pressure

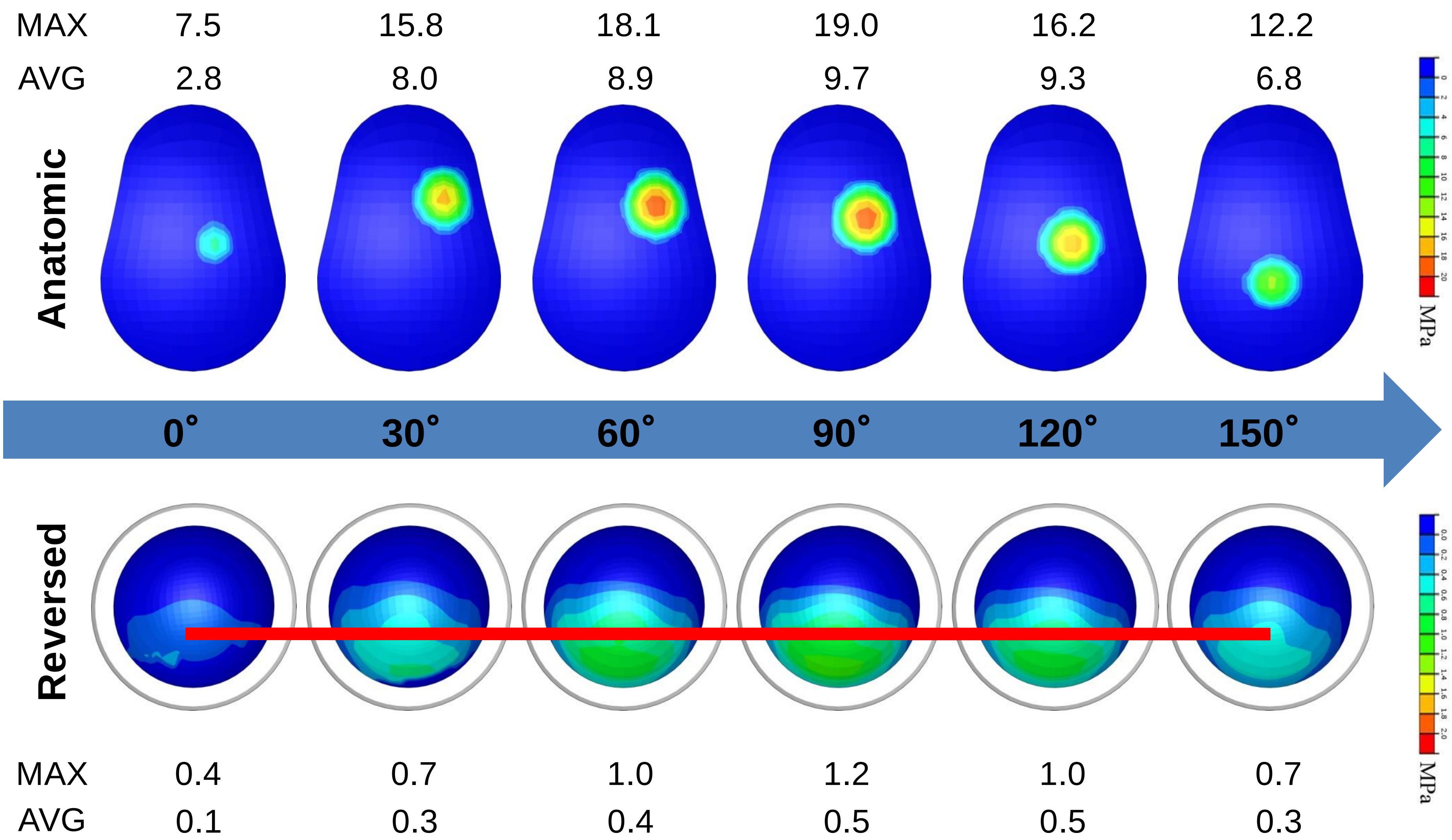

Results: contact pressure

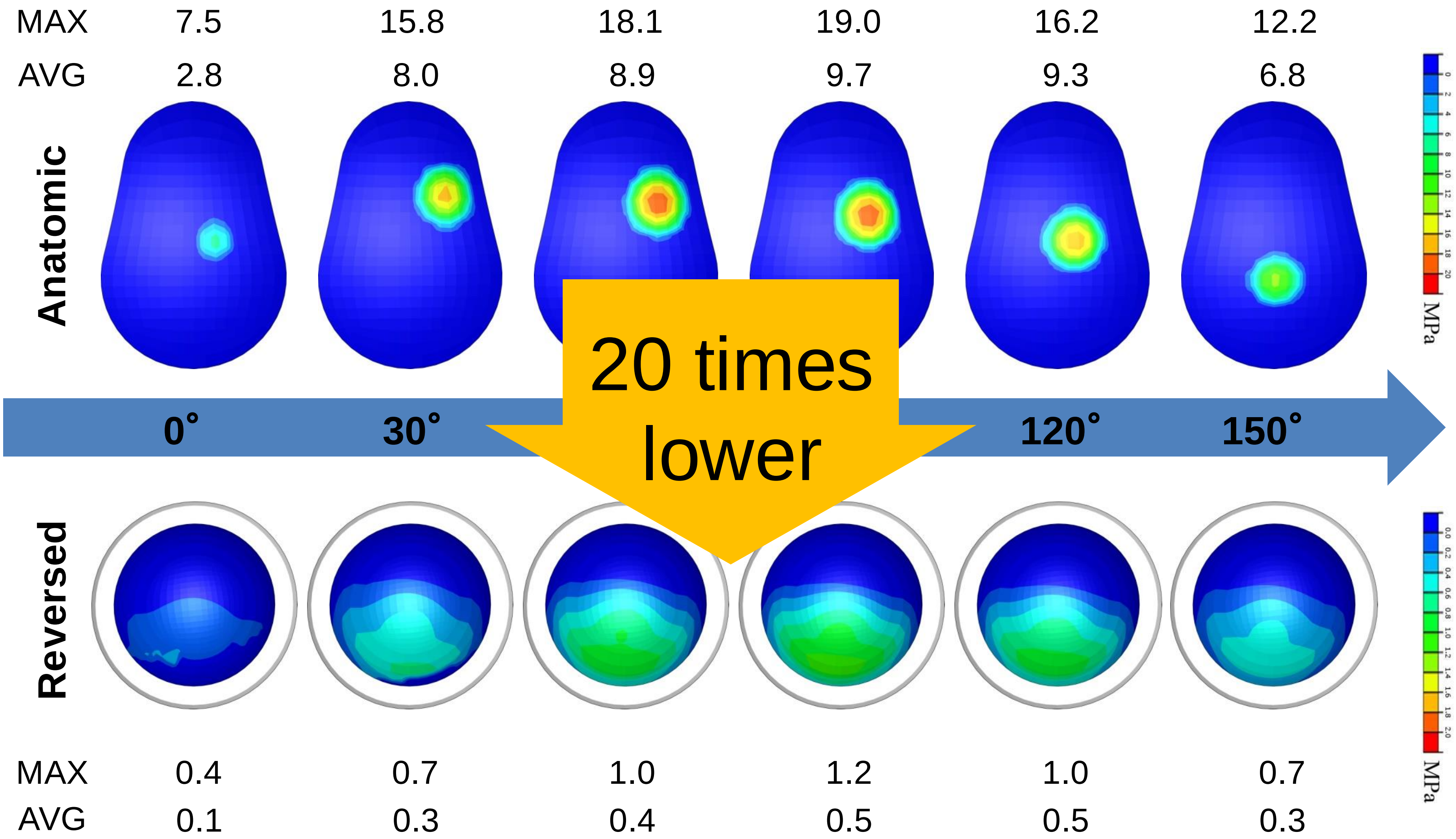

Polyethylene wear

Pressure + Sliding

Polyethylene wear

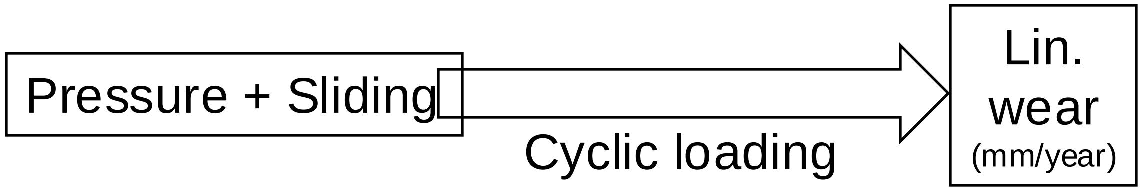

Polyethylene wear

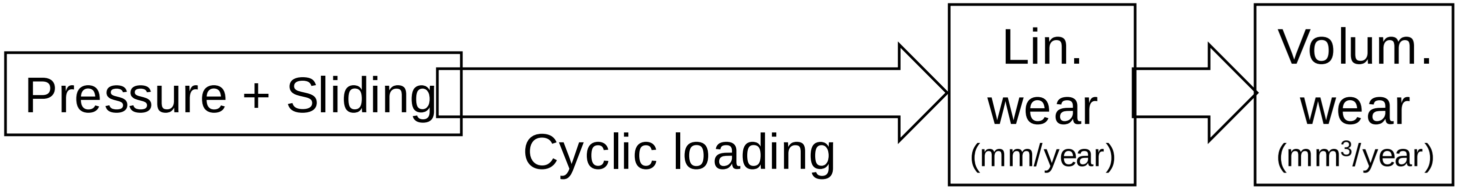

Polyethylene wear

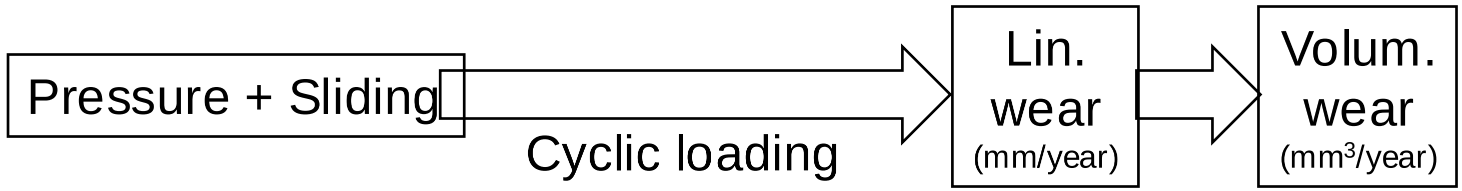

Archard law $H_c = \int k(p)\, p\, ds$

Polyethylene wear

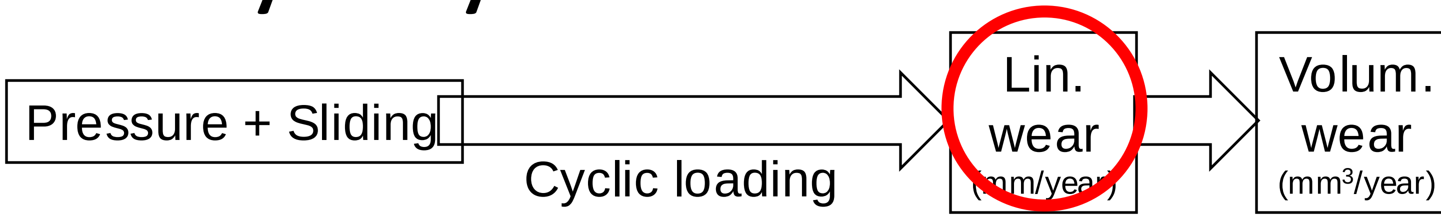

Archard law $H_c = \int k(p)\, p\, ds$

Polyethylene wear

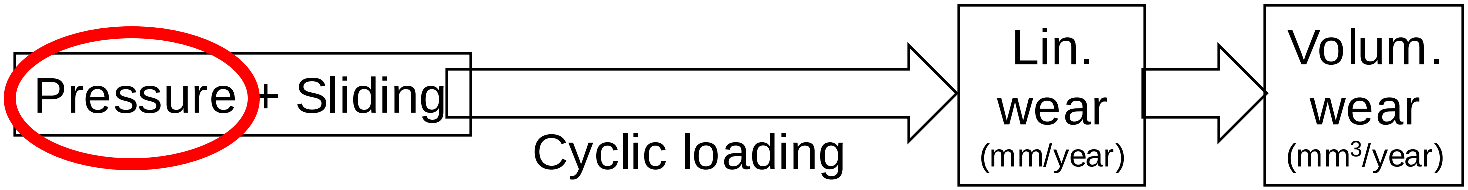

Archard law $H_c = \int k(p)\, p\, ds$

Polyethylene wear

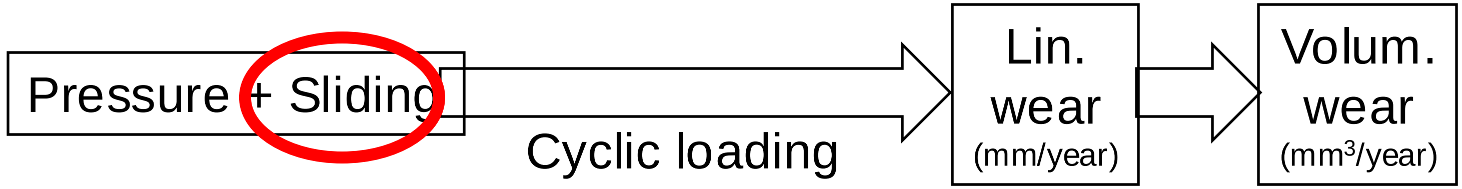

Archard law $H_c = \int k(p)\, p\, ds$

Polyethylene wear

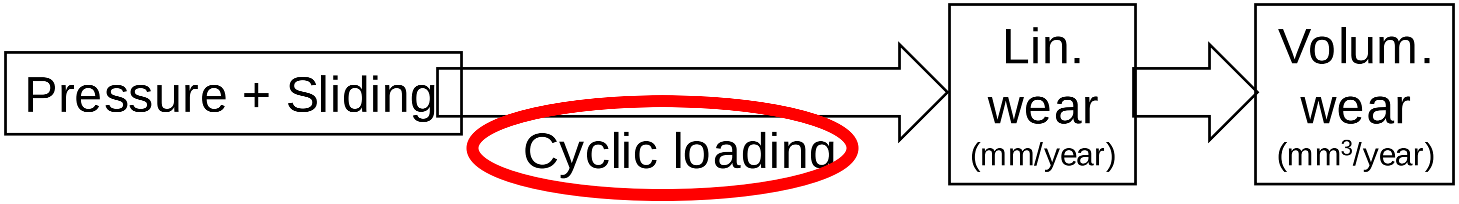

$$\text{Archard law } H_c = \int k(p)\, p\, ds$$

Polyethylene wear

Pressure + Sliding → Cyclic loading → Lin. wear (mm/year) → Volum. wear (mm^3/year)

Archard law $H_c = \int k(p)\, p\, ds$

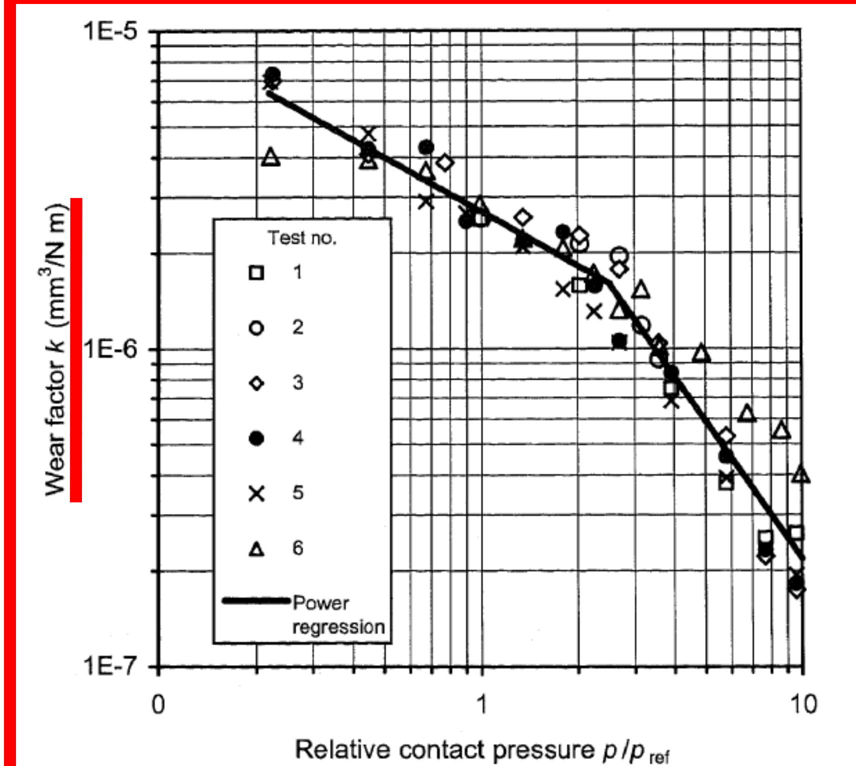

Saikko 06

Polyethylene wear

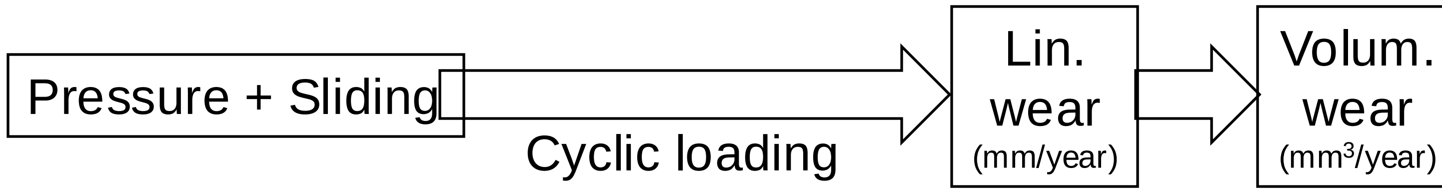

Polyethylene wear

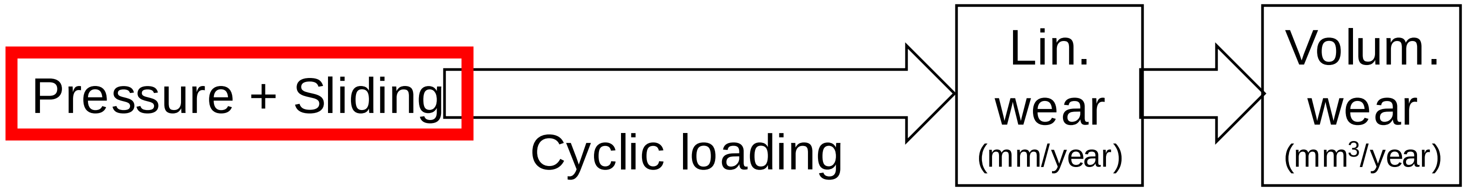

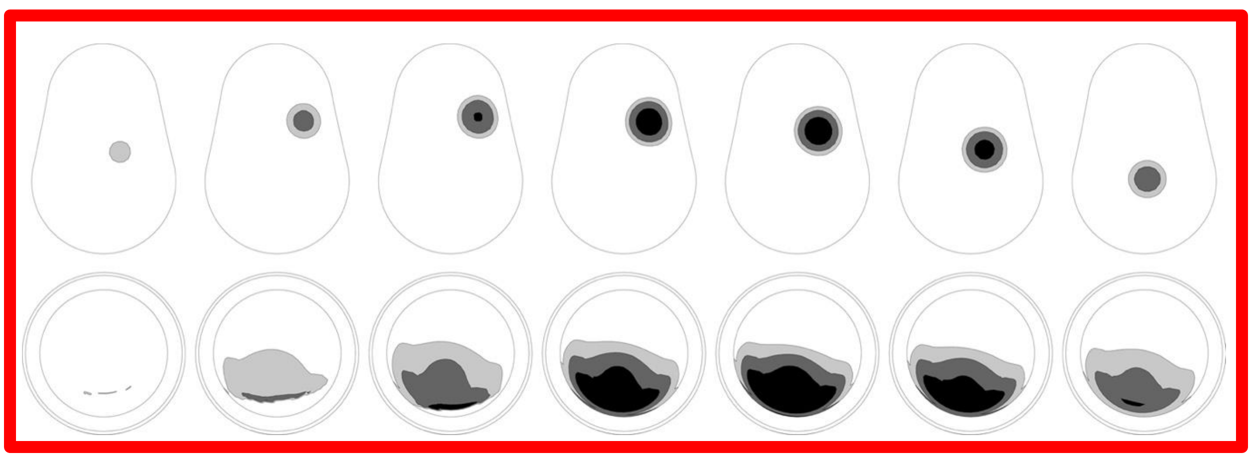

Polyethylene wear

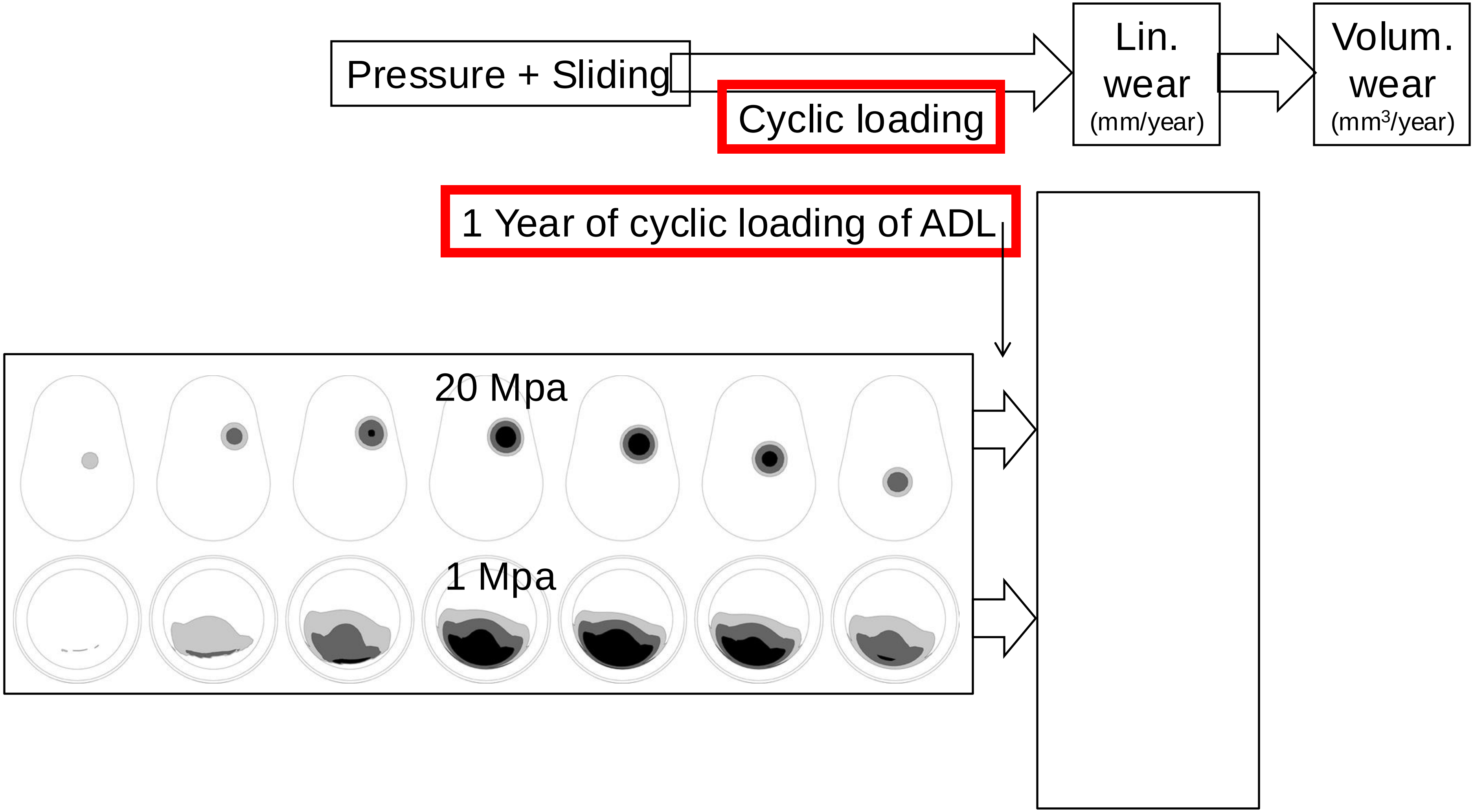

Polyethylene wear

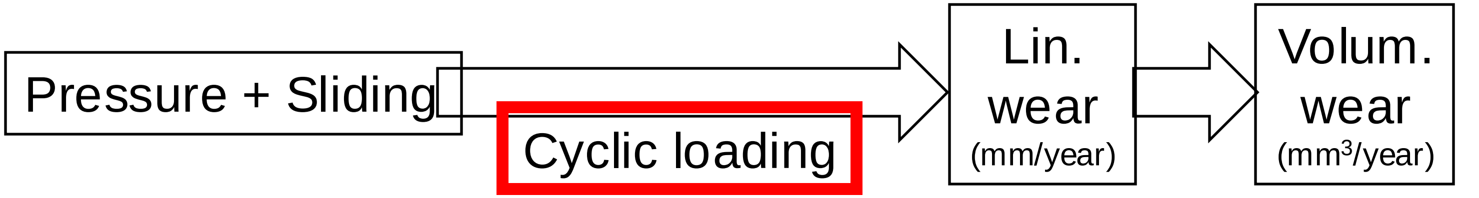

1 Year of cyclic loading of ADL

Abduction level (degree)	10	30	50	70	90	110	130	150
Daily frequency	13021	6790	5557	2678	633	153	34	37

Brian Coley (EPFL-LMAM)

Polyethylene wear

Pressure + Sliding → Cyclic loading → Lin. wear (mm/year) → Volum. wear (mm^3/year)

1 Year of cyclic loading of ADL

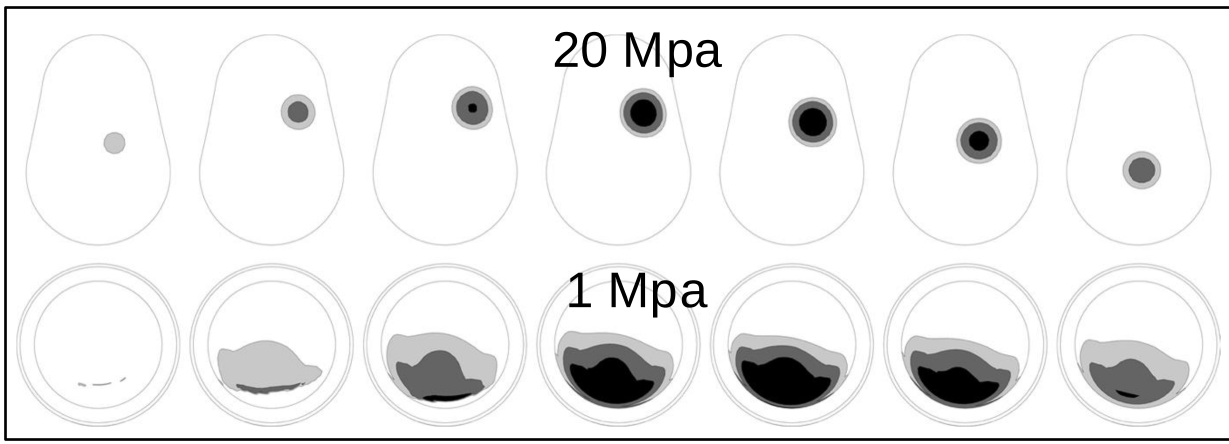

Polyethylene wear

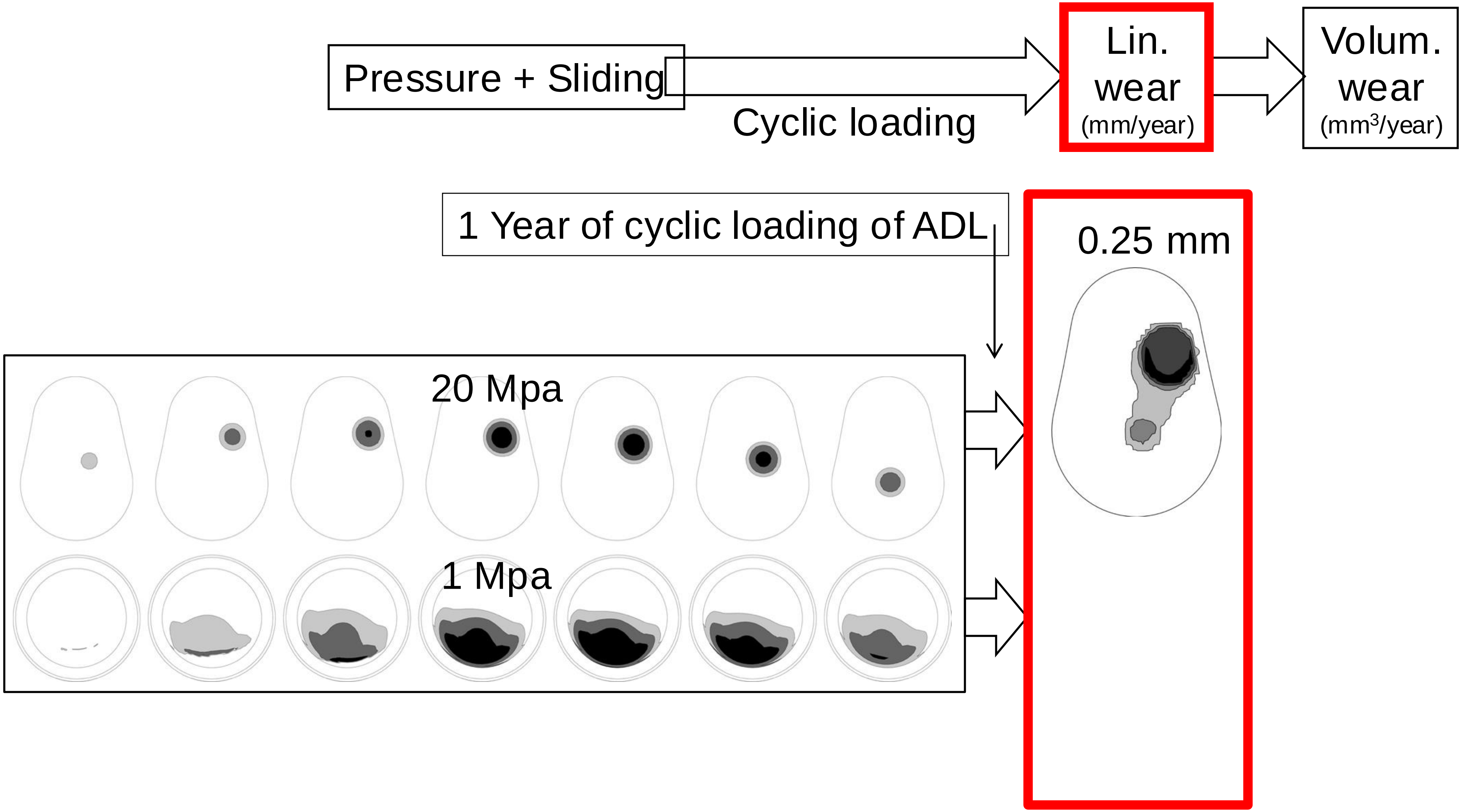

Polyethylene wear

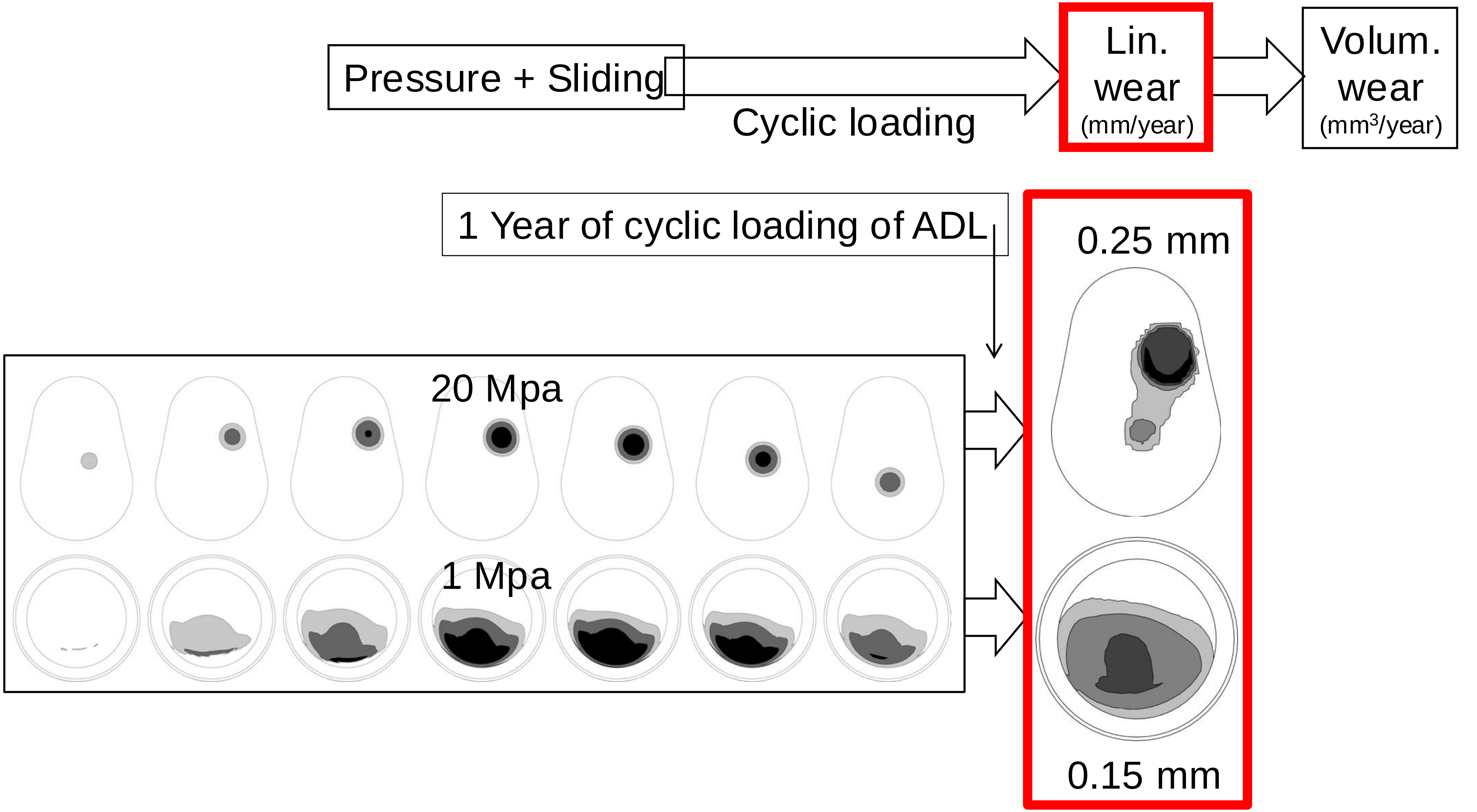

Polyethylene wear

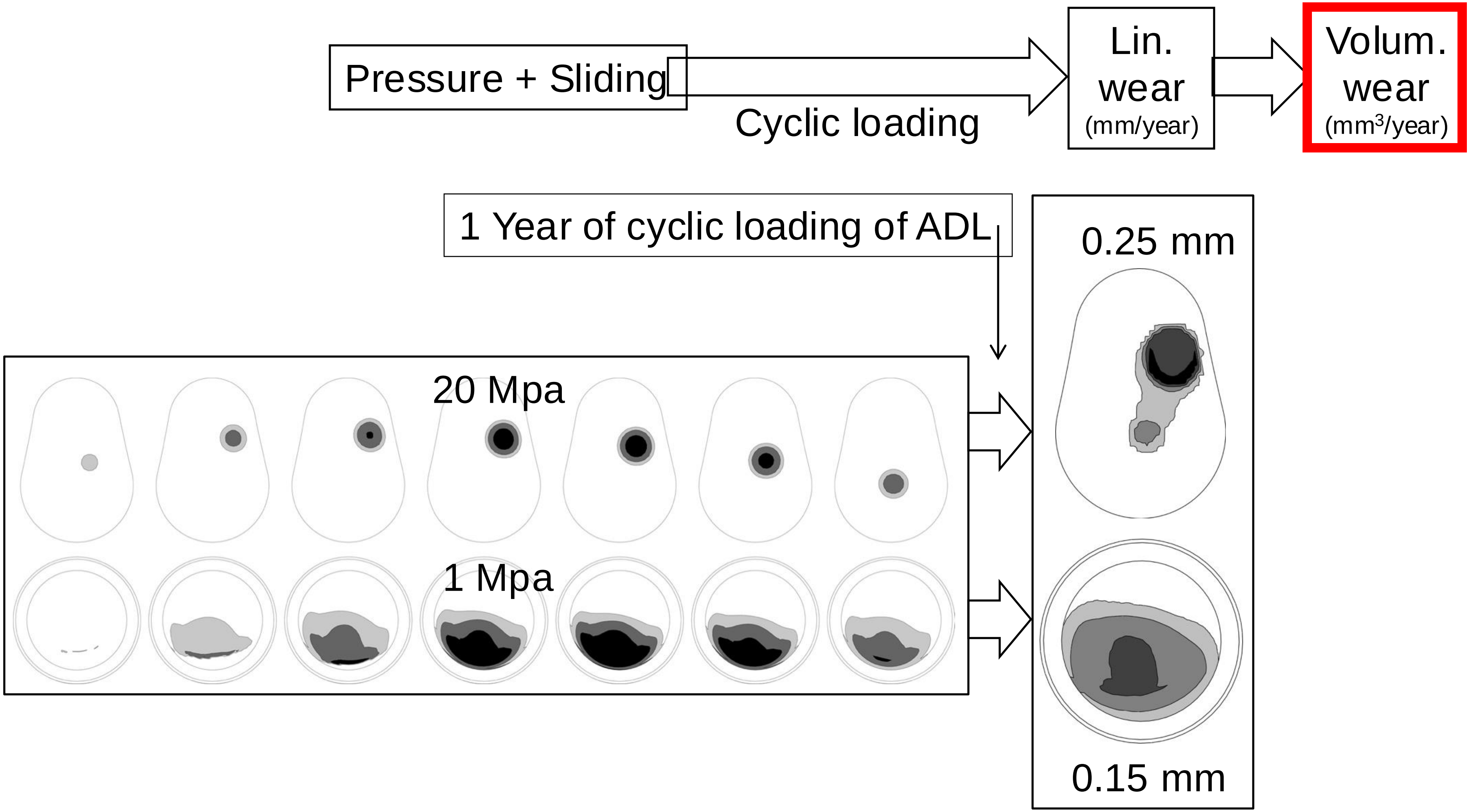

Polyethylene wear

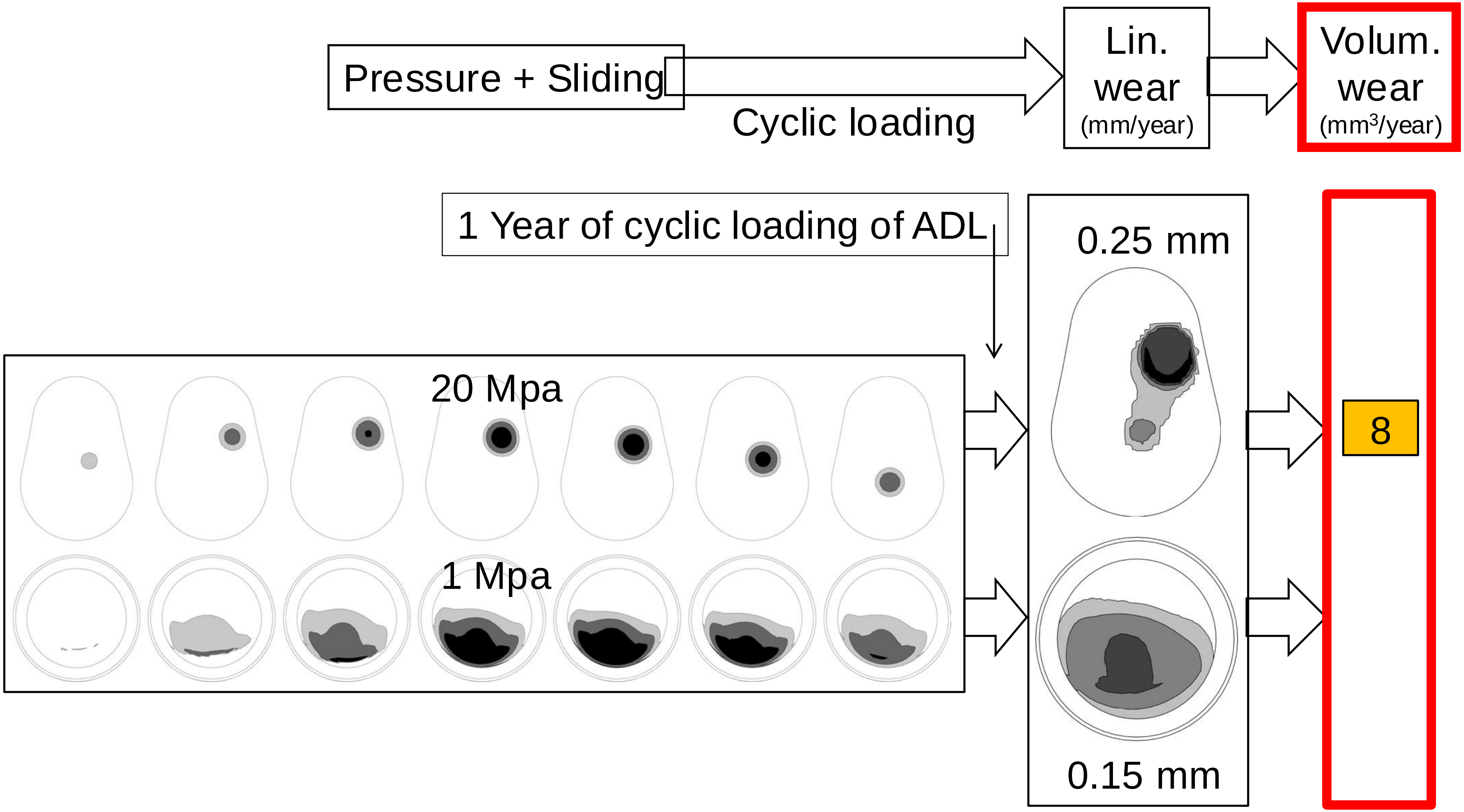

Polyethylene wear

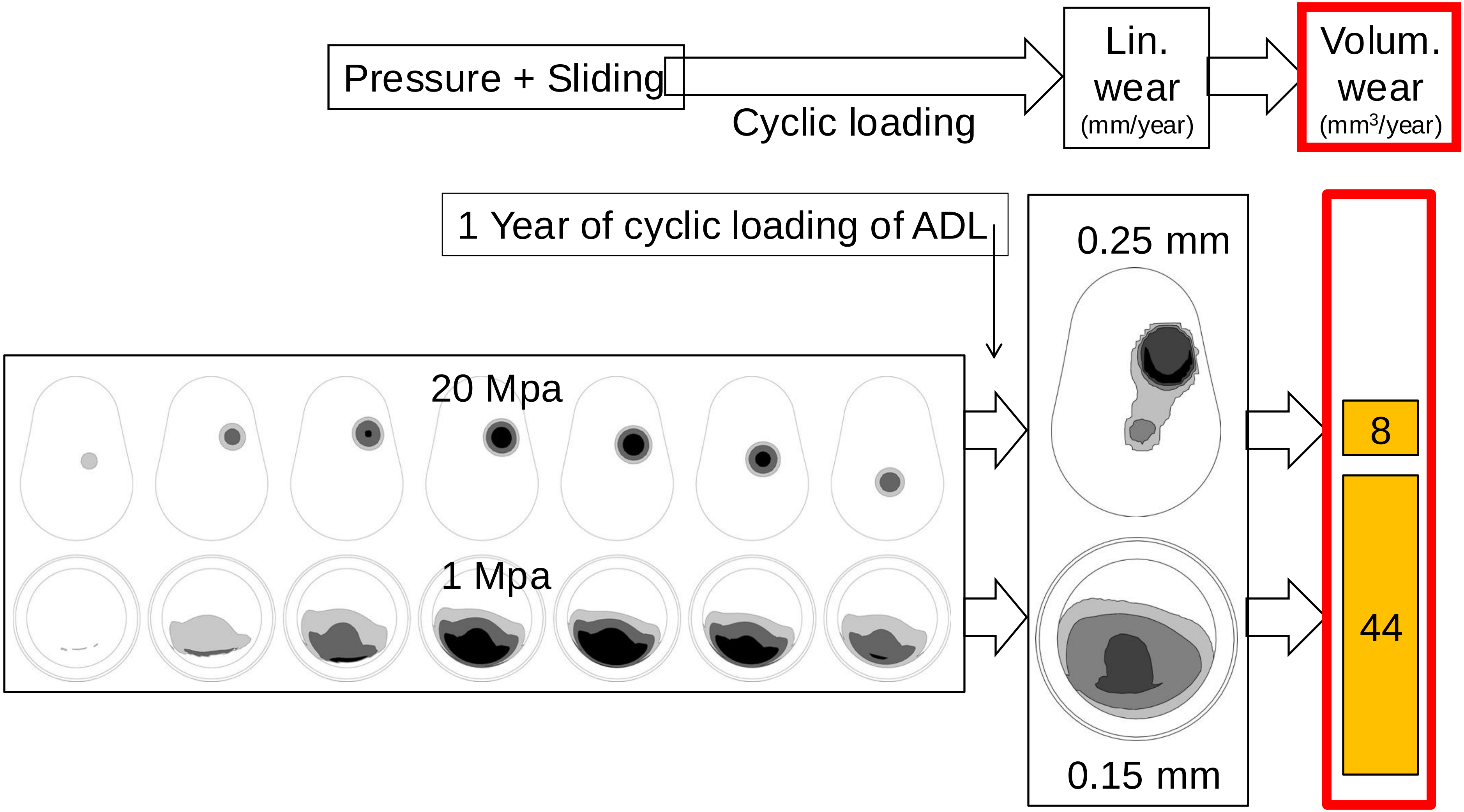

Polyethylene wear

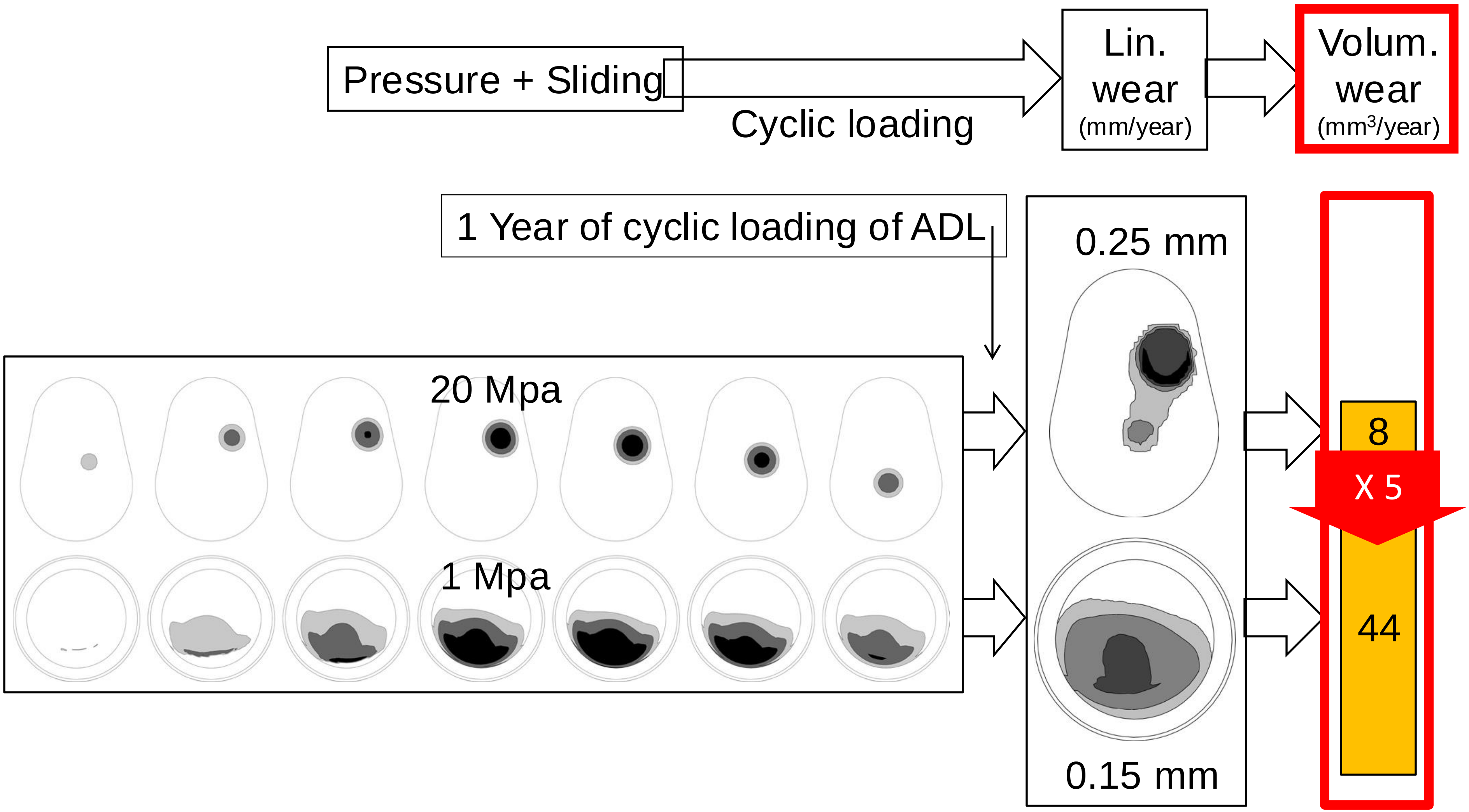

Comparison with clinics

Journal of Shoulder and Elbow Surgery

In vivo volumetric and linear wear measurement of reverse shoulder arthroplasty at minimum 5-year follow-up

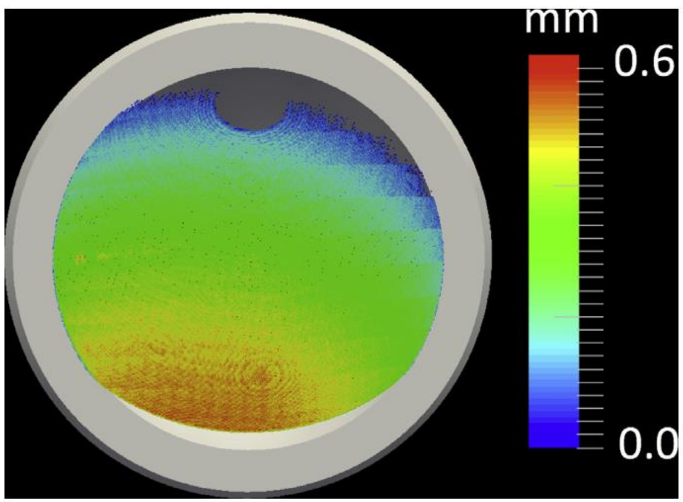

Figure 2 Wear map from neutral arm position (subject No. 07). Linear wear depth is visualized by the color bar, measured in millimeters. The unworn semicircle in the superior quadrant of the liner is the location of the glenosphere screw hole at the time of imaging.

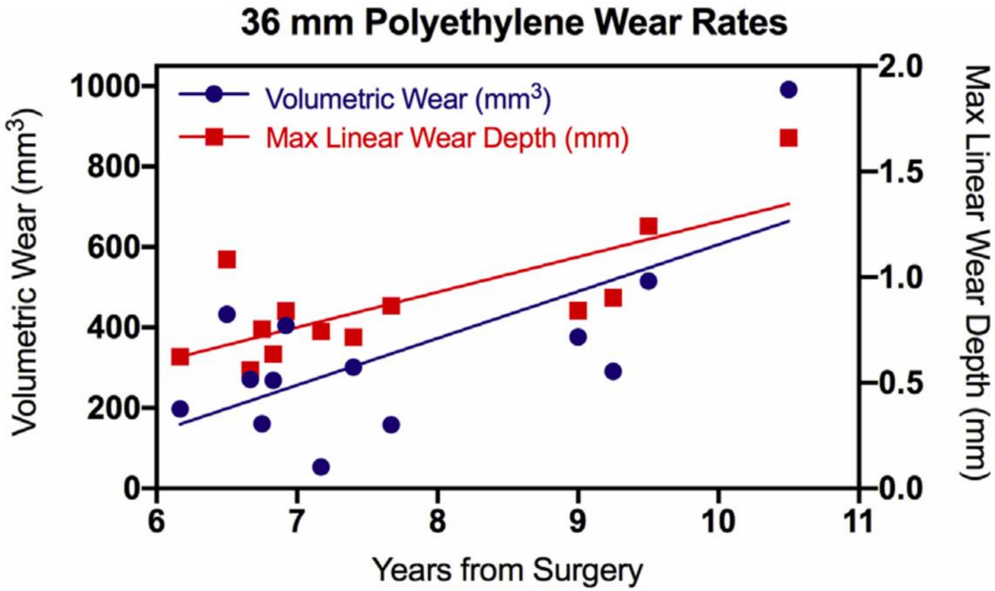

Figure 4 Volumetric (■) and linear (●) wear measurements for each 36-mm polyethylene liner. *Max*, maximum.

J Shoulder Elbow Surg (2020) 29, 1695–1702

Glenoid bone quality

Clinical Background

- Glenohumeral osteoarthritis
- Total shoulder arthroplasty
- Cemented Glenoid implant
- Glenoid Loosening (33% @ 9 yrs)
- Bone support importance

Kasten et al, JBJS-B, 2010

Objectives

1. Glenoid bone quality from preoperative CT
2. Predict cement stress by FE model
3. Correlation between bone quality and cement stress
4. Apply on patients planed for TSA

Methods: Patients

- Inclusion criteria
  - Primary osteoarthritis
  - Planned for anatomical TSA
- Exclusion criteria
  - Rotator cuff tears
  - Fractures
- 20 patients
- Age: 72 years (54 – 88)
- Sex: 15 women + 5 men

Methods: Cement Stress

Patient-specific Finite Element model

- Abduction in the scapular plane
- Allow humerus translations
- Controlled by muscles
  - Anterior, middle, posterior deltoid
  - Subscapularis, supraspinatus, infraspinatus

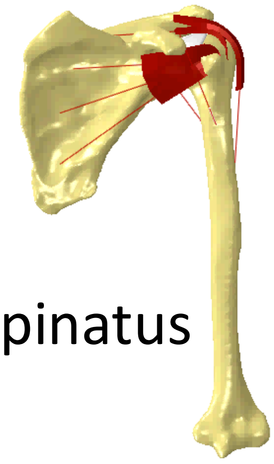

Terrier et al., Clin Biomech, 2014, 28(2): 146-150.

Methods: Cement Stress

Patient-specific parameters: (from CT)

- Bone geometry (scapula + humerus)
- Glenoid bone elasticity (inhomogeneous)
- Muscles: direction and cross-section
- Total shoulder arthroplasty planning

Methods: Cement Stress

Total Shoulder Arthroplasty planning:

- Aequalis PerForm keeled (Tornier)
- Implant positioned within 5° of scapular axis
- Optimal bone support
- Verified by experienced shoulder surgeon
- Uniform (elastic) cement layer (0.5 mm)

Methods: Cement Stress

Volume of cement above critical stress

- 60 degrees of abduction
- Maximum principal stress (tension)
- Critical stress:
  - 1 MPa
  - **3 MPa**
  - 5 MPa

Method: Correlations

Cement stress vs. glenoid bone quality

- Volume of cement above 3 values of critical stress
- Average bone quality (HU) in 7 ROIs
- Evaluated on 20 patients
- Simple correlations
- Combined correlations (cortical & trabecular)
- Coefficient of determination R^2 and p-value

Results: Cement Stress

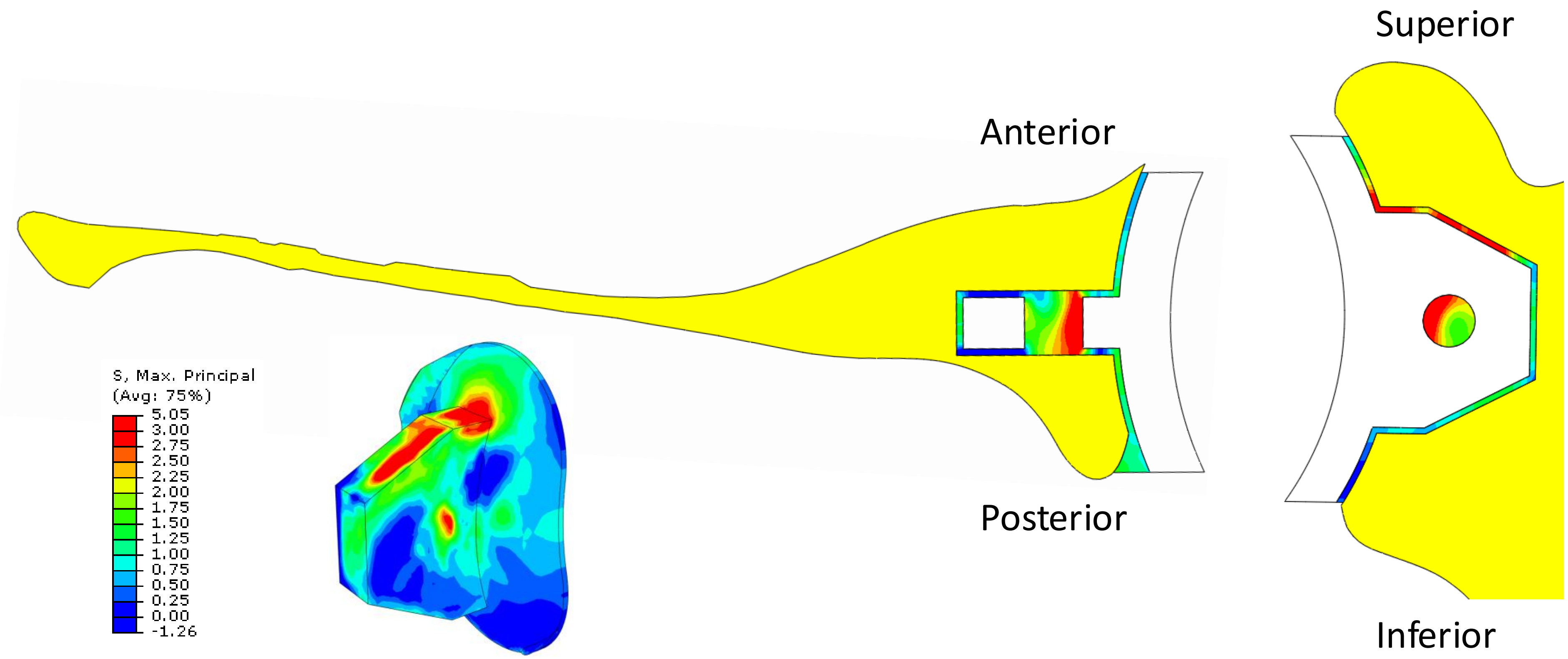

Cement stress predictions after anatomic total shoulder arthroplasty are correlated with preoperative glenoid bone quality

J Shoulder Elbow Surg (2017) 26, 1644–1652

Journal of Shoulder and Elbow Surgery

Patients: 7♀ & 13♂ matched for age & BMI

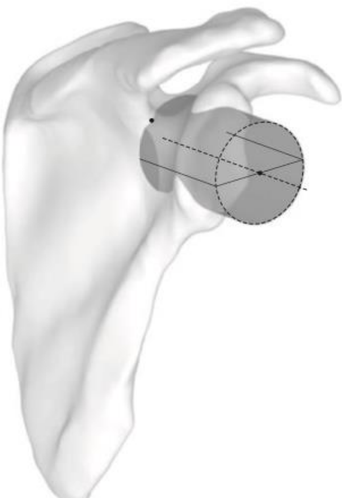

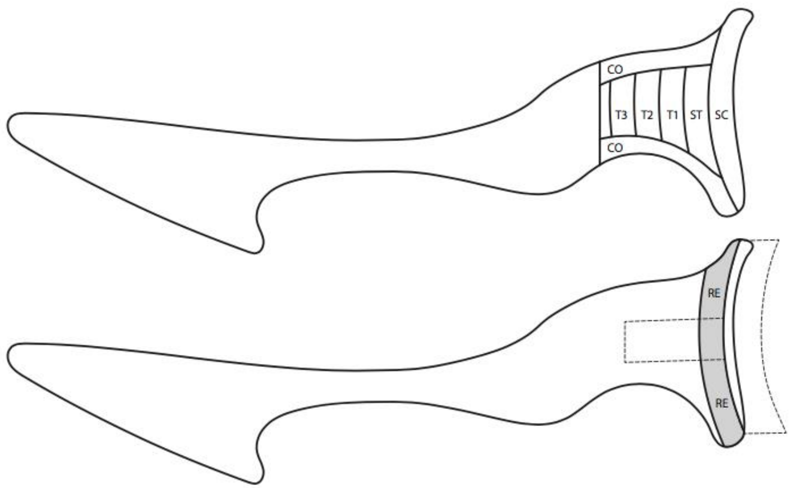

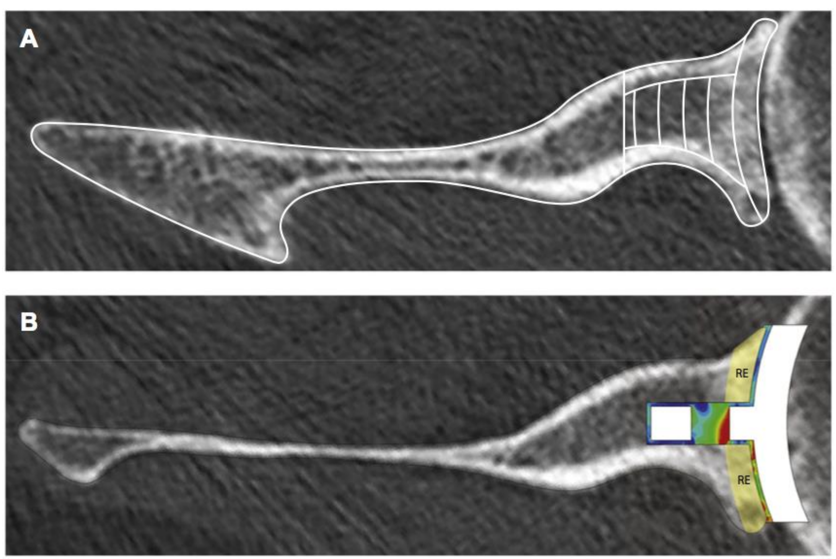

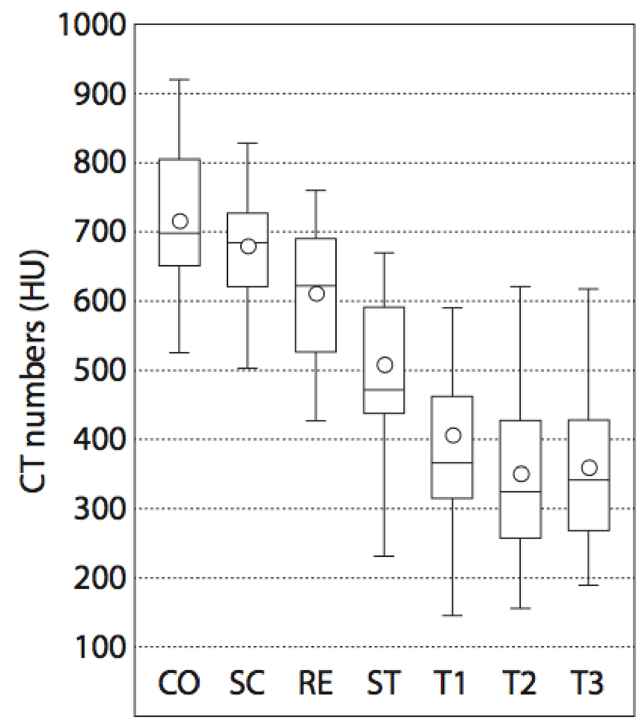

Cement stress predictions after anatomic total shoulder arthroplasty are correlated with preoperative glenoid bone quality

J Shoulder Elbow Surg (2017) 26, 1644–1652

Journal of Shoulder and Elbow Surgery

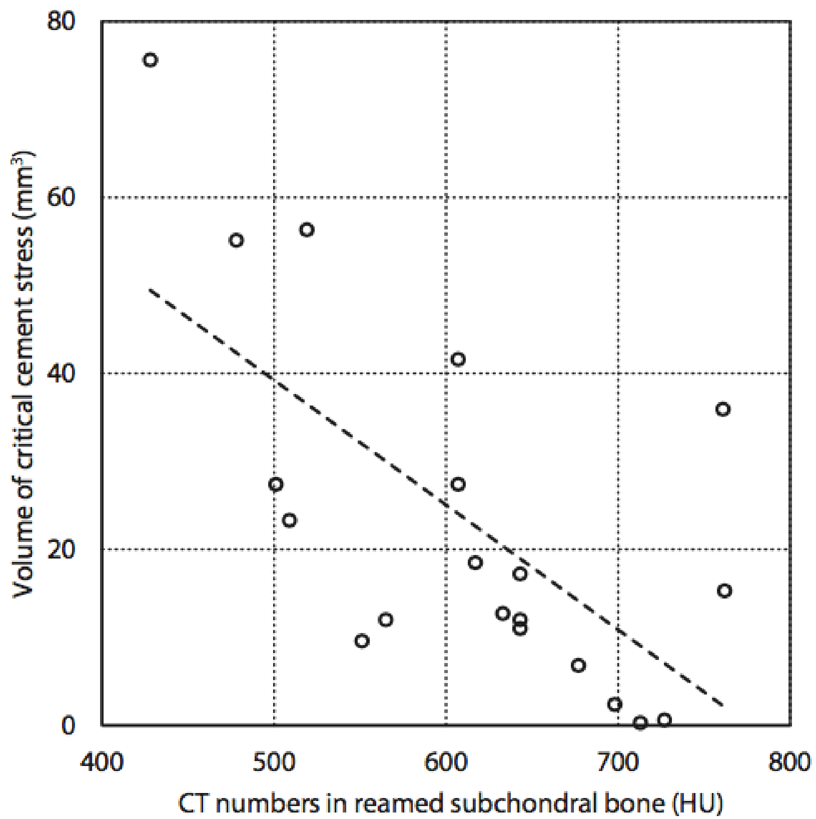

Table I Pearson correlation coefficients (*r*) and associated *P* values between finite element predictions of cement stress, bone-cement interfacial stress, and bone strain and preoperative glenoid bone quality in 7 different volumes of interest

	Cement stress		Bone-cement interfacial stress		Bone strain	
	r	*P*	*r*	*P*	*r*	*P*
CO	−0.412	.071	−0.488	.029	−0.559	.010
SC	−0.180	.447	0.006	.980	−0.359	.120
RE	−0.660	.002	−0.282	.227	−0.531	.016
ST	−0.634	.003	−0.597	.005	−0.614	.004
T1	−0.510	.022	−0.577	.008	−0.468	.037
T2	−0.500	.025	−0.577	.008	−0.460	.041
T3	−0.444	.050	−0.583	.007	−0.456	.044

CO, cortical bone; RE, subchondral bone after reaming; SC, subchondral cortical plate; ST, subchondral trabecular bone; T1-T3, successive adjacent layers of trabecular bone.

Conclusion

- Preserve glenoid (subchondral) bone quality
- Importance of preoperative planning
- Bone quality measure in preoperative planning
- Augmented glenoid implants

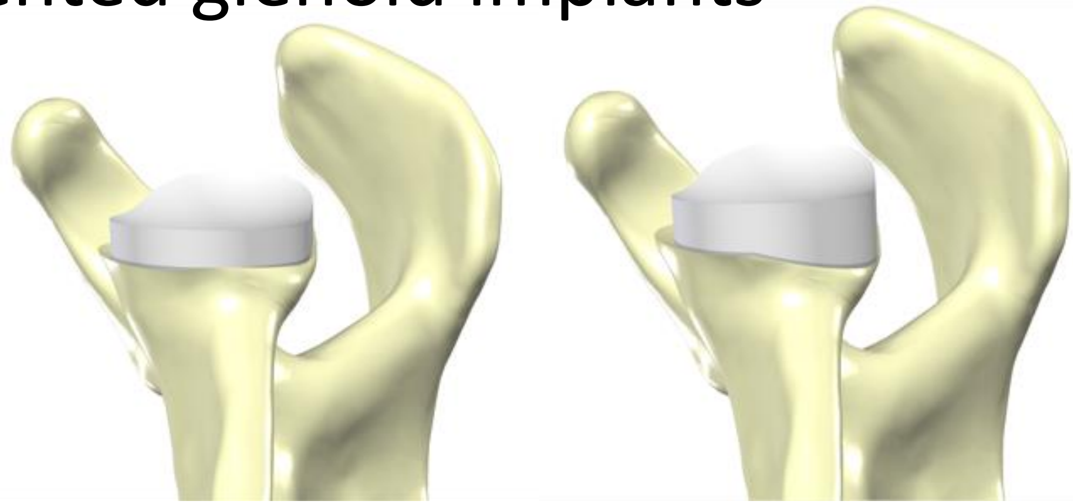

Standard Augmented

Experimental validation

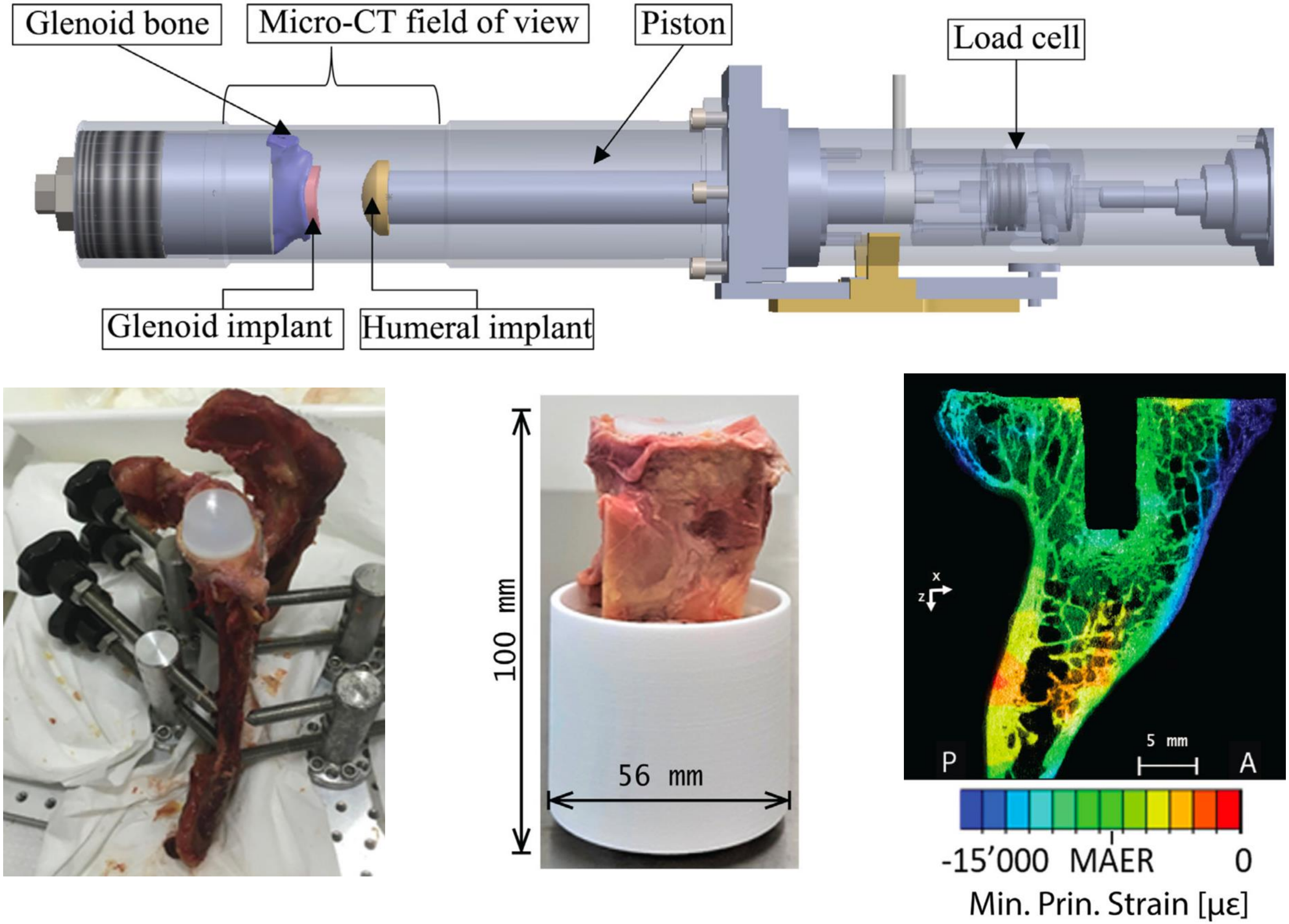

Y. Boulanaache, F. Becce, A. Farron et al. / Medical Engineering and Physics 85 (2020) 48–54

Link with clinical reality

- 262 patients reviewed retrospectively (CHUV)
- 135 patients included
- 2 groups, matched for 2 years follow-up, age, gender, MBI, Walch class
  - No loosening (CTR): 59
  - Loosening (LSG): 26

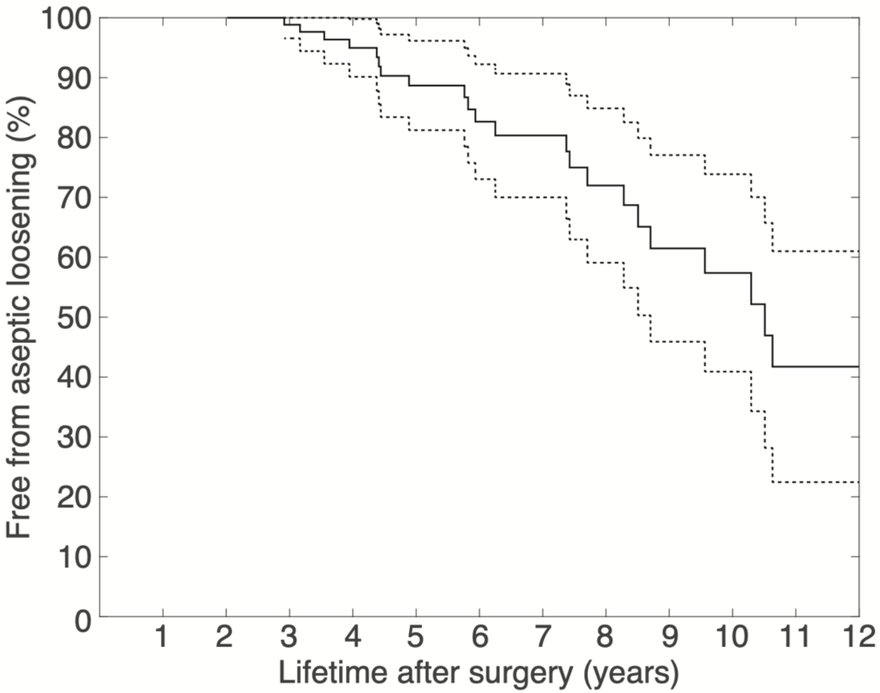

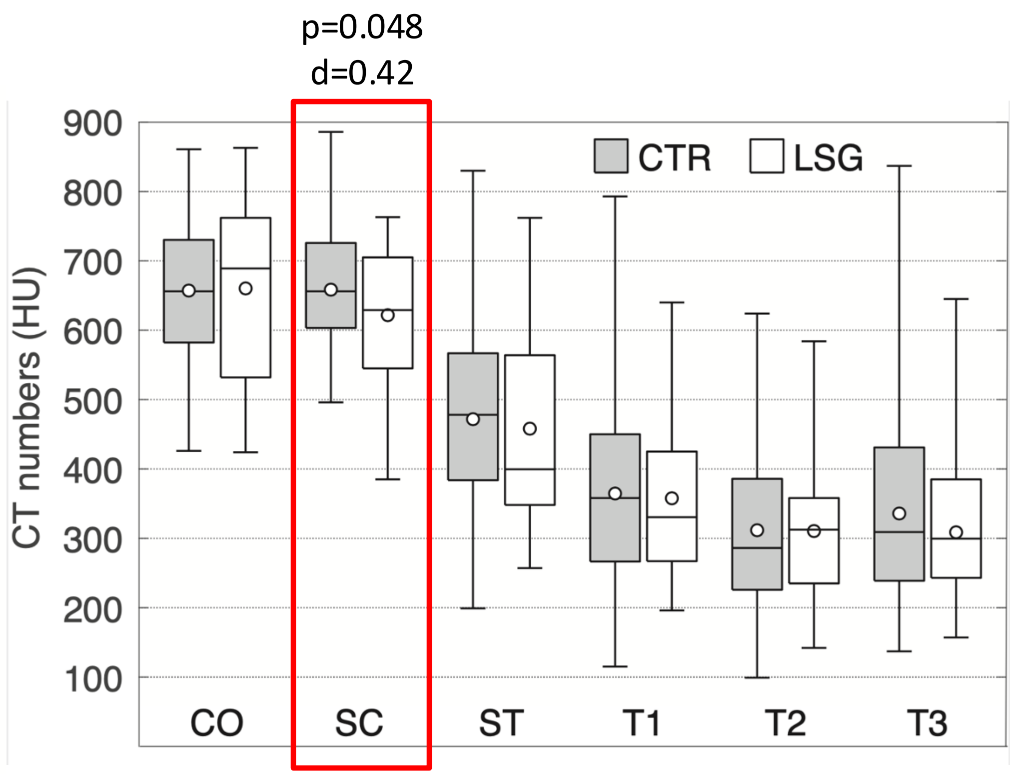

→ Slight differences in bone quality ($p=0.048$) with medium effect size ($d=0.42$)

Critical Shoulder Angle

THE BONE & JOINT JOURNAL

Is there an association between the individual anatomy of the scapula and the development of rotator cuff tears or osteoarthritis of the glenohumeral joint?

A RADIOLOGICAL STUDY OF THE CRITICAL SHOULDER ANGLE

B. K. Moor,
S. Bouaicha,
D. A. Rothenfluh,
A. Sukthankar,
C. Gerber

VOL. 95-B, No. 7, JULY 2013

Osteoarthritis:
28.1° (18.6° to 35.8°)
Control:
33.1° (26.8° to 38.6°)
Rotator cuff tear:
38.0° (29.5° to 43.5°)

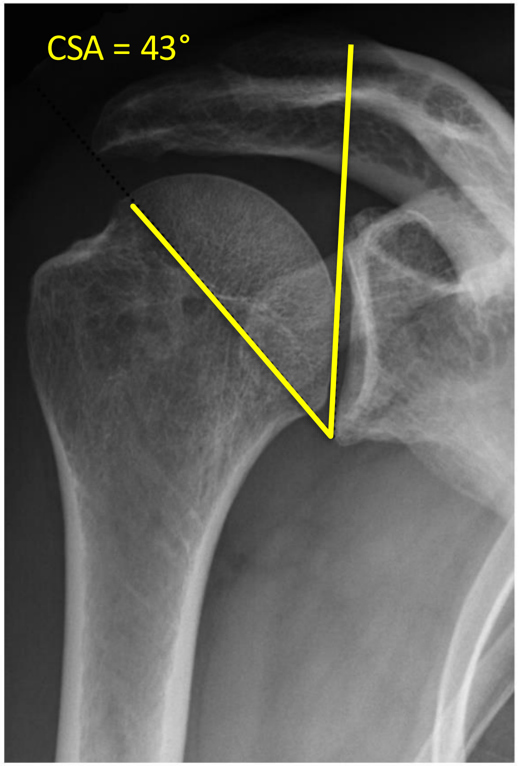

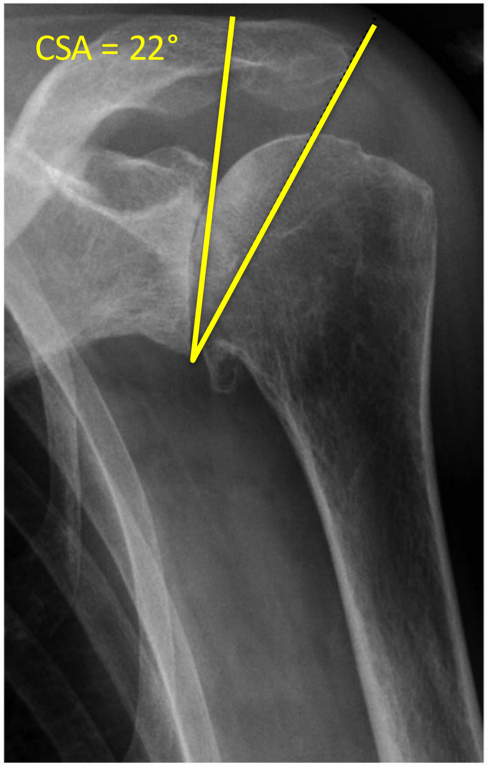

Critical Shoulder Angle

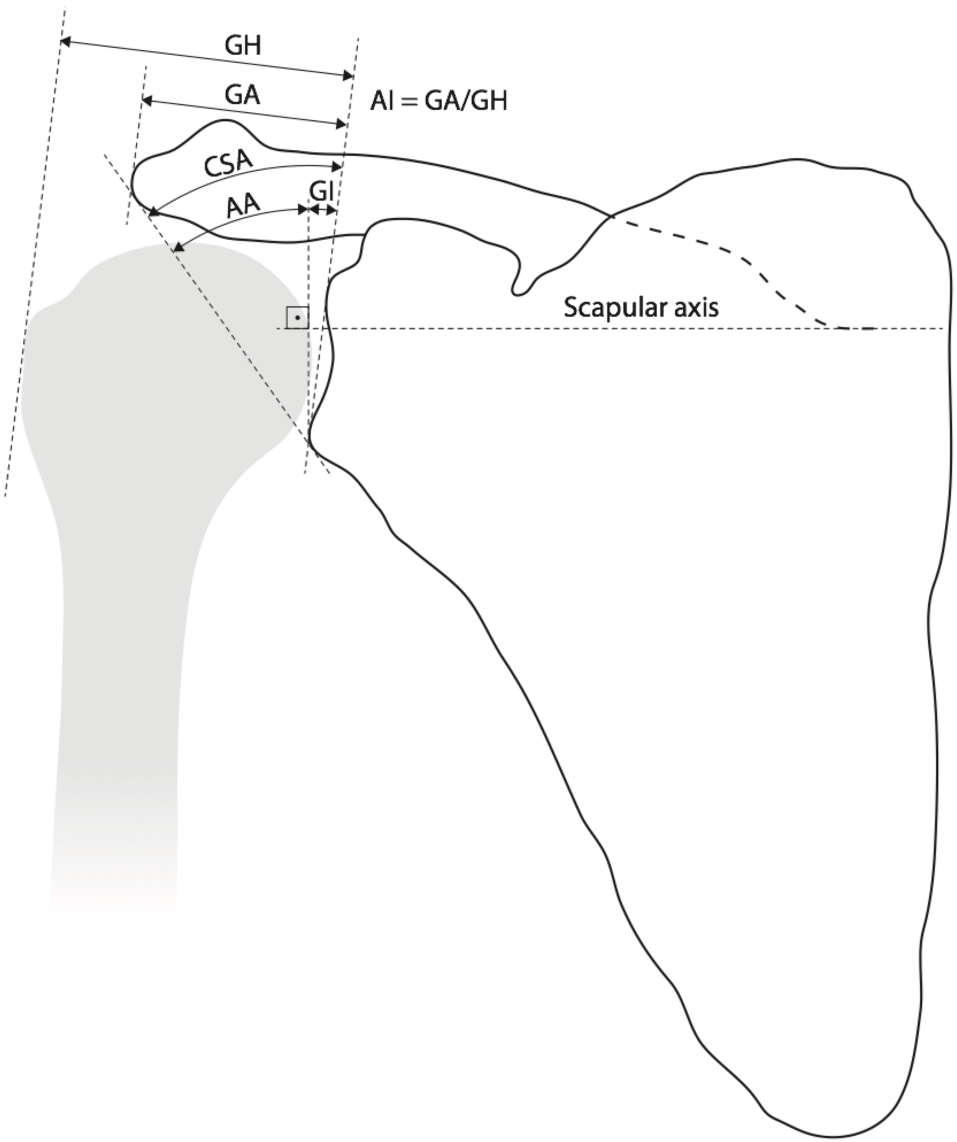

CSA > control → Tendon tear

→ Humerus migration?

CSA < control → Cartilage degeneration

→ Cartilage strain ?

Musculoskeletal model

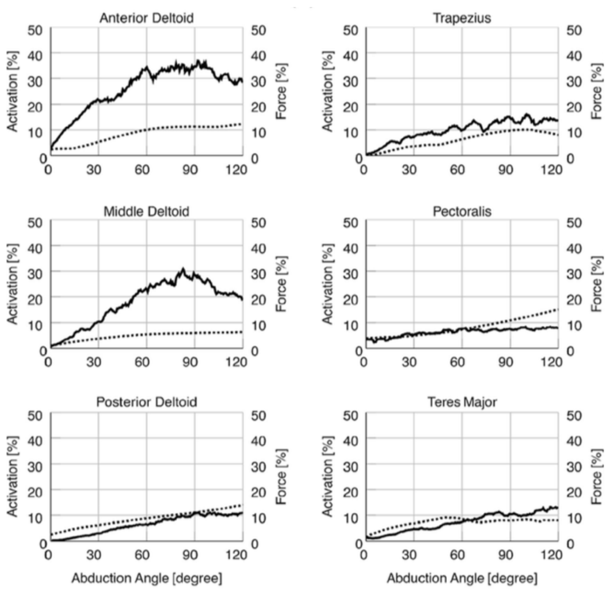

Ingram & Engelhardt (2016)

Critical Shoulder Angle

49 virtual shoulders

7 glenoid inclinations x 7 acromion indexes

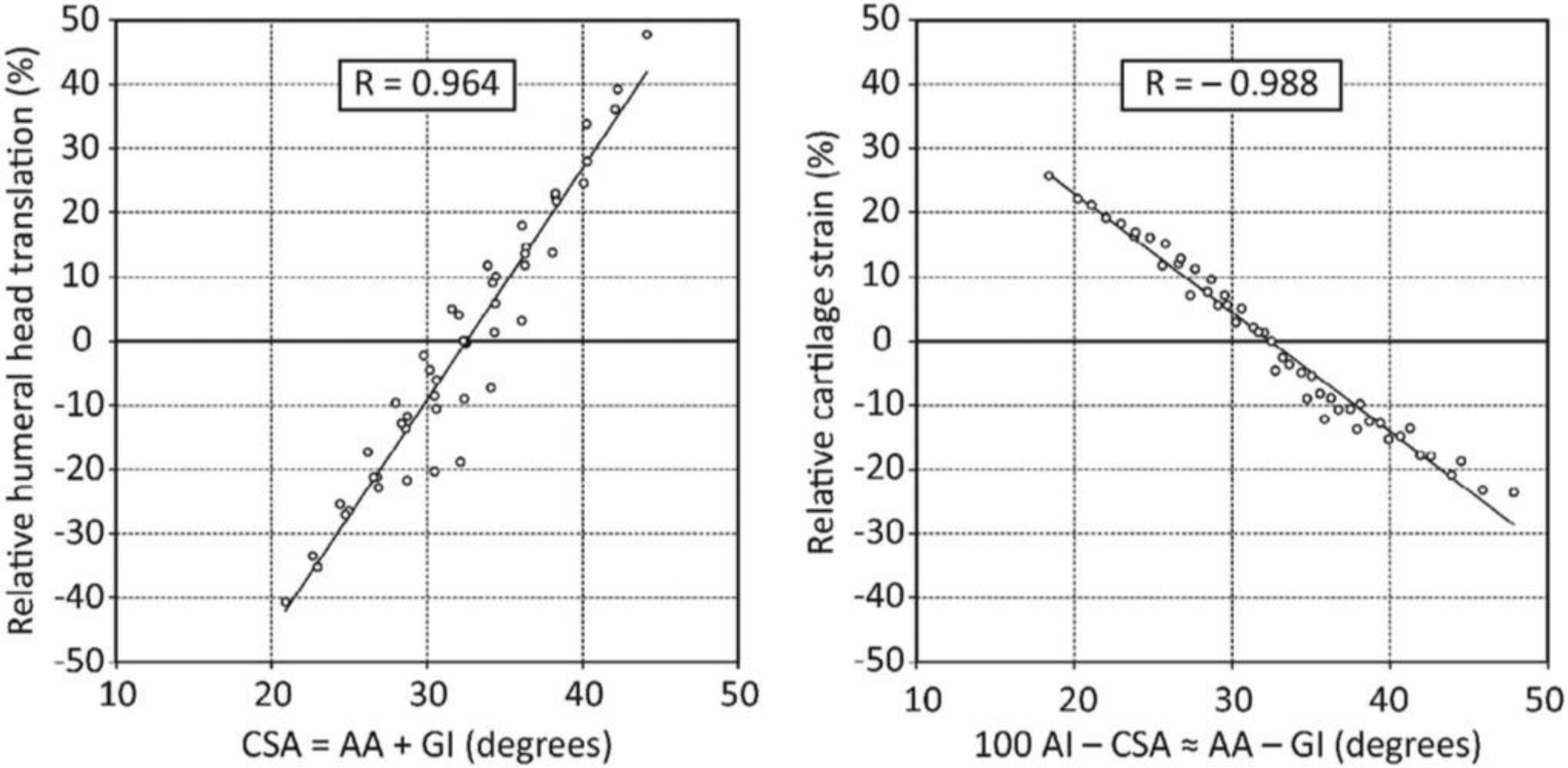

Engelhardt C, Farron A, Becce F, Place N, Pioletti DP, Terrier A. Effects of glenoid inclination and acromion index on humeral head translation and glenoid articular cartilage strain. Journal of Shoulder and Elbow Surgery. 2017;26(1):157–64.

Patient repository for statistical analyses